Elsevier Editorial System(tm) for Marine Micropaleontology
Manuscript Draft

Manuscript Number:

Title: Discorhabdus as a key coccolith genus for paleoenvironmental reconstructions (Middle Jurassic, Lusitanian Basin): biometry and taxonomic status

Article Type: Research Paper

Keywords: Discorhabdus; Biometry; Late Aalenian-Early Bajocian; Middle Jurassic

Corresponding Author: Dr. Gatsby-Emperatriz López-Otálvaro, Ph.D

Corresponding Author's Institution: University Lyon 1

First Author: Gatsby-Emperatriz López-Otálvaro, Ph.D

Order of Authors: Gatsby-Emperatriz López-Otálvaro, Ph.D; Baptiste Suchéras-Marx, PhD student; Fabienne Giraud, PhD; Emanuela Mattioli, PhD; Christophe Lécuyer, PhD

Abstract: This study affords new information about biometric characterization of Discorhabdus coccoliths during the early mid-Jurassic, a period characterized by the onset of oceanic spreading of the North-Atlantic Ocean and western Tethys and a subsequent major paleoceanographic change. The biometric variation of Discorhabdus coccoliths is thoroughly studied in an attempt to understand their relationship with paleoenvironmental conditions in the Lusitanian Basin (west Portugal). Biometric analyses were outlined from a set of 29 samples taken from the marl/limestone couplets of the reference section of Cabo Mondego, Late Aalenian to Early Bajocian in age.
Sizes of the largest (L) and shortest (l) axes of distal and proximal shields, and of central area of Discorhabdus are determined with a Light Microscope based upon random measurements of specimens using natural and polarized lights. Three species of Discorhabdus are differentiated: Discorhabdus striatus, Discorhabdus ignotus and Discorhabdus criotus; D. striatus being the largest form, and D. ignotus and D. criotus the smallest ones. Mixture analysis reveals a bimodal pattern where the biometric boundary of the distal shield averages at mean L axis of 5 μm. An increase in Discorhabdus size occurred from the Late Aalenian to the Early Bajocian due to a raise in size of the whole Discorhabdus's pool and in the abundance of D. striatus. We propose that increasing sizes in Discorhabdus are associated with paleoproductivity as supported by the rising of total nannofossil accumulation rates and by d13C data from the Cabo Mondego section. However, the Discorhabdus size pattern may also represent a response to changes in sea-surface temperatures, or to an evolutionary trend. Previous stable isotope studies from several Mediterranean Tethyan settings have evidenced a relatively warmth of oceanic temperatures during the studied interval at a supra-regional scale rather than at a local level. Rise of sea temperatures may have thus influenced such an increase in abundances of D. striatus as well as the size of Discorhabdus' pool. Our results additionally demonstrated that the Discorhabdus size increase matches the history of calcareous nannofossil turnover (radiation, diversity and increasing abundances) during the Middle Jurassic exemplifying the Cope's rule.

Abstract

This study affords new information about biometric characterization of *Discorhabdus* coccoliths during the early mid-Jurassic, a period characterized by the onset of oceanic spreading of the North-Atlantic Ocean and western Tethys and a subsequent major paleoceanographic change. The biometric variation of *Discorhabdus* coccoliths is thoroughly studied in an attempt to understand their relationship with paleoenvironmental conditions in the Lusitanian Basin (west Portugal). Biometric analyses were outlined from a set of 29 samples taken from the marl/limestone couplets of the reference section of Cabo Mondego, Late Aalenian to Early Bajocian in age.

Sizes of the largest (L) and shortest (l) axes of distal and proximal shields, and of central area of *Discorhabdus* are determined with a Light Microscope based upon random measurements of specimens using natural and polarized lights. Three species of *Discorhabdus* are differentiated: *Discorhabdus striatus*, *Discorhabdus ignotus* and *Discorhabdus criotus*; *D. striatus* being the largest form, and *D. ignotus* and *D. criotus* the smallest ones. Mixture analysis reveals a bimodal pattern where the biometric boundary of the distal shield averages at mean L axis of 5 μm. An increase in *Discorhabdus* size occurred from the Late Aalenian to the Early Bajocian due to a raise in size of the whole *Discorhabdus*'s pool and in the abundance of *D. striatus*. We propose that increasing sizes in *Discorhabdus* are associated with paleoproductivity as supported by the rising of total nannofossil accumulation rates and by $\delta^{13}C$ data from the Cabo Mondego section. However, the *Discorhabdus* size pattern may also represent a response to changes in sea-surface temperatures, or to an evolutionary trend. Previous stable isotope studies from several Mediterranean Tethyan settings have evidenced a relatively warmth of oceanic temperatures during the studied interval at a supra-regional scale rather than at a local level. Rise of sea temperatures may have thus influenced such an increase in abundances of *D. striatus* as well as the size of *Discorhabdus*' pool. Our results

additionally demonstrated that the *Discorhabdus* size increase matches the history of calcareous nannofossil turnover (radiation, diversity and increasing abundances) during the Middle Jurassic exemplifying the Cope's rule.

Cover Letter

Gatsby-Emperatriz LOPEZ-OTALVARO
UMR CNRS 5276 Laboratoire de Géologie de Lyon
Université Claude Bernard Lyon 1
27-43 Boulevard 11 Novembre 1918
69622 Villeurbanne Cedex, France
E-mail: gatsbyemperatriz@usal.es

Villeurbanne, July 25th, 2011

Dear editors of *Marine Micropaleontology*

Please find enclosed a manuscript untitled "*Discorhabdus* as a key coccolith genus for paleoenvironmental reconstructions (Middle Jurassic, Lusitanian Basin): biometry and taxonomic status", that my colleagues Baptiste Suchéras-Marx, Fabienne Giraud, Emanuela Mattioli, Christophe Lécuyer and I submit to *Marine Micropaleontology*.

In this paper, for the first time, we perform biometric analyses of Middle Jurassic *Discorhabdus* (coccolithophore). These analyses allow us to clarify the taxonomic status of *Discorhabdus*, and show that the size of this taxon can be used as a paleoenvironmental proxy.

We include here the body of the manuscript (LOPEZ-OTALVARO_ETAL.doc), 5 figures (.eps) and 3 tables (.eps).

As requested, we propose four names of potential referees: Miriam Cobianchi (**miriam@unipv.it**), Elisabetta ERBA (**elisabetta.erba@unimi.it**), Paul BOWN (**p.bown@ucl.ac.uk**) and Jeremy YOUNG (**j.young@nhm.ac.uk**)

Sincerely yours,

Gatsby-Emperatriz LOPEZ-OTALVARO

Research Highlights

- Middle Jurassic *Discorhabdus* (coccolith) show a bimodal size frequency
- A 5 µm mean length of the distal shield discriminates among species of *Discorhabdus*
- Changes in *Discorhabdus* sizes can be used as a paleoenvironmental proxy

Discorhabdus as a key coccolith genus for paleoenvironmental reconstructions (Middle Jurassic, Lusitanian Basin): biometry and taxonomic status

Gatsby-Emperatriz López-Otálvaro[a*], Baptiste Suchéras-Marx[a], Fabienne Giraud[a,b], Emanuela Mattioli[a], Christophe Lécuyer[a]

[a]UMR 5276 - CNRS Laboratoire de Géologie de Lyon : Terre, Planètes, Environnement, Université Lyon 1, ENS Lyon, Bâtiment Géode, 2 rue Raphaël Dubois, F-69622 Villeurbanne cedex, France

[b]present adress: ISTerre, UMR 5275, Université de Grenoble 1, 1381 rue de la Piscine, BP 53, 38041 Grenoble cedex 9, France

*Corresponding author: Gatsby-Emperatriz López-Otálvaro, gatsbyemperatriz@usal.es

Abstract

This study affords new information about biometric characterization of *Discorhabdus* coccoliths during the early mid-Jurassic, a period characterized by the onset of oceanic spreading of the North-Atlantic Ocean and western Tethys and a subsequent major paleoceanographic change. The biometric variation of *Discorhabdus* coccoliths is thoroughly studied in an attempt to understand their relationship with paleoenvironmental conditions in the Lusitanian Basin (west Portugal). Biometric analyses were outlined from a set of 29 samples taken from the marl/limestone couplets of the reference section of Cabo Mondego, Late Aalenian to Early Bajocian in age.

Sizes of the largest (L) and shortest (l) axes of distal and proximal shields, and of central area of *Discorhabdus* are determined with a Light Microscope based upon random measurements of specimens using natural and polarized lights. Three species of *Discorhabdus* are differentiated: *Discorhabdus striatus*, *Discorhabdus ignotus* and *Discorhabdus criotus*; *D. striatus* being the largest form, and *D. ignotus* and *D. criotus* the smallest ones. Mixture

analysis reveals a bimodal pattern where the biometric boundary of the distal shield averages at mean L axis of 5 μm. An increase in *Discorhabdus* size occurred from the Late Aalenian to the Early Bajocian due to a raise in size of the whole *Discorhabdus*'s pool and in the abundance of *D. striatus*. We propose that increasing sizes in *Discorhabdus* are associated with paleoproductivity as supported by the rising of total nannofossil accumulation rates and by $\delta^{13}C$ data from the Cabo Mondego section. However, the *Discorhabdus* size pattern may also represent a response to changes in sea-surface temperatures, or to an evolutionary trend. Previous stable isotope studies from several Mediterranean Tethyan settings have evidenced a relatively warmth of oceanic temperatures during the studied interval at a supra-regional scale rather than at a local level. Rise of sea temperatures may have thus influenced such an increase in abundances of *D. striatus* as well as the size of *Discorhabdus*' pool. Our results additionally demonstrated that the *Discorhabdus* size increase matches the history of calcareous nannofossil turnover (radiation, diversity and increasing abundances) during the Middle Jurassic exemplifying the Cope's rule.

1. Introduction

The Middle Jurassic witnesses a major paleogeographical change related with the oceanic spreading of the western Tethys and the central North-Atlantic Ocean (Mougenot et al., 1979; Ribeiro et al., 1979; Wilson, 1988; Bill et al., 2001). The opening of new connections produced a reassessment of ocean circulation and a major paleoceanographic adjustment that, finally, triggered a significant turnover in marine biota (e.g. Morris, 1982; Morris and Coleman, 1989; Henriques et al., 1994; Sandoval et al., 2001, 2002; Aguado et al., 2008; Sandoval et al., 2008).

Such is the case of radiolarian diversification (Bartolini et al., 1996; 1999; Aguado et al., 2008); radiation of new families and genera of ammonites (O'Dogherty et al., 2006); a

significant faunal turnover of foraminifers (Canales and Henriques, 2008) recorded in the course of the Aalenian-Bajocian, as well as the rapid radiation and increasing abundance of calcareous nannofossils (Cobianchi et al., 1992; Mattioli and Erba, 1999; Aguado et al., 2008) and change in species-specific dominance in nannofossil assemblage (Henriques et al., 1994; Cresta and Pavia, 1994; Pavia and Enay, 1997; Mattioli and Erba, 1999). This biotic revolution also matches a positive $\delta^{13}C$ excursion measured in marine carbonates (Bartolini et al. 1996; Bartolini and Cecca 1999; Bartolini et al., 1999; Morettini et al., 2002; O'Dogherty et al., 2006; Sandoval et al., 2008) and in terrestrial organic matter (Hesselbo et al., 2003) that witness the onset of a global carbon cycle perturbation and a rearrangement of the trophic conditions in western Tethys**.**

Besides radiation within nannofossils, these organisms also experienced a significant change in size (Cobianchi et al., 1992) that has not been yet quantified for the Late Aalenian-Early Bajocian. The application of biometrics to paleoceanographic and paleoclimatic studies has revealed as an outstanding proxy (among the others, Bollmann, 1997; Bornemann et al., 2003; Henderiks and Pagani, 2007; Erba et al., 2010). In Jurassic studies, biometrics on nannofossils have been used for taxonomic purposes, coccolith carbonate paleo-fluxes, paleoenvironmental, paleoceanographic and paleoclimatic reconstructions (Mattioli and Pittet, 2002; Tremolada and Erba, 2002; Bornemann et al., 2003; Mattioli et al., 2004a, b; Giraud et al., 2006; Suan et al., 2008; 2010; Tiraboschi and Erba, 2010; Suchéras-Marx et al., 2010; Fraguas and Erba, 2010). A biometric approach has already been applied to the Family Biscutaceae that is a significant component of the Mesozoic assemblages (Mattioli and Pittet, 2002; Mattioli et al., 2004b; Bornemann and Mutterlose, 2006; Erba et al., 2010), but biometric parameters of this family have not yet been investigated in the Aalenian-Bajocian interval.

Our paper focuses on the biometric analysis of *Discorhabdus*, a genus of the Family Biscutaceae first occurring during the Early Jurassic (Bown, 1987a; Bown and Cooper, 1998; Mattioli and Erba, 1999). The paleoecological affinities of *Discorhabdus* for meso/eutrophic conditions in surface waters are supported by different authors (e.g. Premoli Silva et al., 1989; Erba, 1991; Coccioni et al., 1992; Herrle, 2003; Herrle et al., 2003; Giraud et al., 2003; Tremolada et al., 2005; Mattioli et al., 2008; Giraud, 2009, Giraud et al., 2009). This genus is represented over Late Aalenian-Early Bajocian, period characterized by enhanced eutrophication (Bartolini and Cecca, 1999; Bartolini et al., 1999; Aguado et al., 2008; Sandoval et al., 2008), by three morpho-species**,** namely *Discorhabdus striatus*, *Discorhabdus ignotus* and *Discorhabdus criotus*.

The Cabo Mondego section is the Global Stratotype Section and Point (GSSP) for the Bajocian Stage, thus it is a prominent representative candidate for our study of *Discorhabdus* biometry. *Discorhabdus* is one of the major components of the coccoliths assemblage in the Cabo Mondego section across the Aalenian/Bajocian since is common (1 specimen/2-10 fields of view) to abundant (1-10 specimen/1 field of view) and shows a reliable and consistent record characterized by a wide range of size (distal shield diameter Length 2.42 µm to 8.58 µm) easily recognized in Light Microscope.

The main goal of our work is to reconstruct the variability of *Discorhabdus* coccolith size in order to:

- Obtain a better taxonomic characterization of *Discorhabdus* morpho-species;
- Understand whether the variability in *Discorhabdus* size depends on intra- or inter-specific changes;
- Test whether these variations are related to paleoceanographic/paleoenvironmental changes (i.e., modifications in the trophic regime, or changes of sea surface temperatures) as revealed by geochemical proxies, or to evolutionary processes.

2. Previous work

In the last decade, various studies have shown that biometry applied to coccoliths, and more generally to calcareous nannofossils, is a valuable tool to:

1) Improve the taxonomy at the species level (e.g. *Biscutum* and *Similiscutum* along the Pliensbachian/Toarcian, Mattioli et al., 2004b; *Watznaueria* during Bajocian/Bathonian, Tiraboschi and Erba, 2010; *Watznaueria britannica* during Late Oxfordian, Giraud et al., 2006; *Biscutum constans* and *Watznaueria barnesiae* during Late Albian, Bornemann and Mutterlose, 2006);

2) Precise the biostratigraphic framework (e.g. *Biscutum* and *Similiscutum* along Pliensbachian/Toarcian, Mattioli et al., 2004b; *Watznaueria communis/Watznaueria barnesiae* during Bajocian/Bathonian, Tiraboshi and Erba, 2010);

3) Better understand their paleoecological preferences to reconstruct paleoceanographic or paleoclimatic conditions (e.g. *Schizosphaerella* over Pliensbachian and Toarcian, Suan et al., 2008, 2010; *Crepidolithus* along Pliensbachian, Suchéras-Marx et al., 2010, Fraguas and Erba, 2010; *Biscutum* and *Similiscutum* during Pliensbachian/Toarcian, Mattioli et al., 2004b; *Watznaueria britannica* in Late Oxfordian, Giraud et al., 2006; *Watznaueria* and nannoliths in Tithonian/Berriasian, Bornemann et al., 2003; *Biscutum constans* and *Watznaueria barnesiae* during Late Albian, Bornemann and Mutterlose, 2006). In addition, accurate reconstruction of coccolith and nannolith size trend has been regarded as a useful proxy to reconstruct carbonate fluxes through time (e.g. *Schizosphaerella* over Pliensbachian/Toarcian, Mattioli and Pittet, 2002; several taxa in Tithonian/Berriasian, Bornemann et al., 2003).

3. Geographic and geologic setting

The marginal Lusitanian Basin, located in western-central Portugal, originated during the onset of oceanic spreading of the North-Atlantic Ocean occurring from the Late Triassic to the Early Cretaceous (Mougenot et al., 1979; Ribeiro et al., 1979; Wilson, 1988; Wilson et al., 1989; Bill et al., 2001) (Fig. 1). The Lusitanian Basin corresponds to a carbonate homoclinal ramp where a thick lithostratigraphical sequence of marls and argillaceous limestones was deposited (Azerêdo et al., 1988; Ruget-Perrot, 1961; Mouterde et al., 1971; 1979). Shallow-water sedimentation took place on the eastern/southeastern part of the basin and gradually changed into deeper-water successions towards the west/northwest (Azerêdo, 1993; Watkinson, 1989).

Cabo Mondego, 200 km north of Lisbon, is located between the Mountain of Boa Viagem, the Mondego River and the beaches of Figueira da Foz and Murtinheira (Ruget-Perrot, 1961) (Fig. 1). The Cabo Mondego section is the Bajocian GSSP (Pavia and Enay, 1997). The marl/limestone alternations are represented over more than 400 meters of succession encompassing the Late Toarcian to Middle Callovian (Rocha et al., 1990). The stratigraphic interval from the Late Aalenian (Concavum ammonite Zone) to the Early Bajocian (Sauzei ammonite Zone) selected for our study is approximately 80 meters thick.

The characteristic fauna of Western Europe is very well represented in the Cabo Mondego section with high abundance of ammonites, belemnites, brachiopods and bivalves (Ruget-Perrot, 1961; Henriques et al., 1994; Pavia and Enay, 1997). Microfossils (foraminifera, dinoflagellates, spores/pollen and calcareous nannofossils) are also common along the section (Henriques et al., 1994; Pavia and Enay, 1997).

We used in this study the biostratigraphic framework of Ruget-Perrot (1961), Rocha et al (1981) and Henriques et al (1994) provided by Tethyan ammonites. Concerning the nannofossil biostratigraphy, Hamilton (1977, 1979) first established a biostratigraphy for the

Callovian in the Cabo Mondego section, and Gardin and Manivit (1991) were also working on biostratigraphy across the Aalenian/Bajocian boundary.

4. Methodology

4.1. Preparation techniques

Twenty nine samples (26 from the marls and 3 from the limestones of the Cabo Mondego section) displaying the best-preserved and abundant nannofossil assemblages were selected for biometric purposes. The Aalenian/Bajocian boundary was oversampled, and then samples were taken at a lower space in the rest of the succession. Thus, smear slides were prepared following two techniques: 1) the random settling technique described by Beaufort (1991) and modified by Geisen et al. (1999), and 2) the standard rippled smear slide procedure (Bown and Cooper, 1998). The first technique allows the quantification of the nannofossil absolute abundance, and then the nannofossil accumulation rates, which is compared to the *Discorhabdus* size trend.

4.2. Taxonomic framework

The morpho-taxonomy of the genus *Discorhabdus* used in this work follows the descriptions of Perch-Nielsen (1968), Moshkovitz and Ehrlich (1976), Bown (1987b) and Reale et al (1992) and only concerns three species that were identified over the Late Aalenian to the Early Bajocian interval: *Discorhabdus striatus, Discorhabdus ignotus* and *Discorhabdus criotus* (Fig. 2). After revision of all available literature, synonymies for the three *Discorhabdus* morpho-species are reported in the Appendix A.

4.3 Preservation

Excellent to poorly preserved *Discorhabdus* coccoliths are observed in samples from the Cabo Mondego section, where etching occurs more often than overgrowth. So, different coccolith preservation classes are qualitatively estimated on the basis of etching and overgrowth according to the method first proposed by Roth and Thierstein (1972) and modified by Roth (1973, 1978):

X: excellent preservation (no etching or overgrowth are observed).

Etching:

E-1: Slight etching: coccoliths can display serrate outlines. Delicate central area structures have been slightly affected by dissolution but they are still preserved.

E-2: Moderate etching: The thinnest specimens are preferentially dissolved; delicate structures are cracked in many individuals; serrate outlines of coccoliths are common.

E-3: Strong dissolution: Dissolution-resistant species and nannofossil fragments are consistently abundant, more delicate forms are rare.

Overgrowth:

O-1: Slight overgrowth. Irregular, secondary growth of crystallites and slight thickening of central area structures.

O-2: Moderate overgrowth. Delicate central structures are commonly overgrown and identification is difficult. Irregular secondary growth of crystallites is common.

Partial etching of some elements of the distal or proximal shields and of the central area is frequent in the larger and smaller coccoliths. Some samples contain poorly-preserved *Discorhabdus* displaying strongly etched or overgrown specimens. Overall preservation is slightly worse in the Late Aalenian, and especially in limestones. Most of the measurements and counts were done in marlstone and argillaceous limestone samples (from 52.3 to 84.6 wt%$CaCO_3$) because of the better preservation and higher specimen abundances compared to

pure limestones. In addition, only specimens characterized by slight to moderate etching or overgrowth were retained for biometry.

4.4. Absolute and relative abundances, and nannofossil accumulation rates

Using a polarized Light Microscope (ZEISS Axioscope 40 at 1000x) up to 300 specimens per sample were counted from a variable number of fields of view over the slides prepared for absolute abundance quantification. The absolute nannofossils and *Discorhabdus* abundances (nannofossils*g^{-1} of rock) were calculated using the formula given by Geisen et al (1999). Relative abundances (percentages) of the genus were calculated with respect to the nannofossils total assemblage to see the variations of the whole *Discorhabdus*'s pool. The nannofossils and *Discorhabdus* absolute abundances and *Discorhabdus* species percentages were compared to the biometric results (Fig. 3).

Absolute abundances were converted into nannofossil accumulation rates (NAR, nannofossils*cm^{-2}*Ma^{-1}, Fig. 3) based on the chronostratigraphic scale of Gradstein et al (2004), and on the biostratigraphic framework provided by ammonites (Ruget-Perrot, 1961; Rocha et al., 1981; Henriques et al., 1994) and calcareous nannofossils of Cabo Mondego Section.

4.5. Biometric analysis

For each sample, two or more slides were prepared and observed following several longitudinal transverses to achieve a number of coccoliths statistically significant for the biometric analysis. Between 30 and 66 well-to-moderately preserved specimens of *Discorhabdus* were measured in a variable number of random fields of view for each sample. *Discorhabdus* images captures were taken with a CCD camera Sony XC-77CE using the MCCamera11 software. Measurements were performed with the Motic Images Plus 2.0

software. The resolution of the camera is ±0.08 µm, which corresponds to the size of one pixel. Two images were taken for each specimen, one in natural light and the second one in polarized light (Fig. 2)

In spite of the fact that *Discorhabdus* is a circular coccolith (Noël, 1965), very slight differences can be observed between measurements of the largest axis (L) and the shortest axis (l). The L and l axes of distal and proximal shields and of central area were measured. Four repeated measurements for each axis on the same coccolith both in polarized and natural lights allowed us to calculate the error of measurements that is ± 1 pixel. As the coccolith outline is better visible in natural light, in the following only measurements acquired in natural light will be presented. The number of radial elements of the distal shield was also counted for each specimen both in natural and polarized light in order to verify the counting of these elements.

Mean, median, minimum and maximum values of the different biometric parameters as well as the standard deviation were computed for each species (Table 1). Furthermore, correlations between L and l axes of distal/proximal shields and central area of *Discorhabdus* were tested (Table 2).

Mixture analysis of *Discorhabdus* coccoliths and central area sizes (Fig. 4) were realized using the PAST software (Hammer et al., 2001) to detect if unimodal or polymodal distributions occur. Mixture analysis is a maximum-likelihood method for identifying the presence of one or several distributions in an initially pooled sample and, estimating their descriptive parameters (Redner and Walker, 1984; Titterington et al., 1985; Harper, 1999).

To characterize the variability of *Discorhabdus* size, we used 25 and 75 percentiles besides mean size data. Then, the percentile results were compared to the relative abundances of *Discorhabdus* to investigate whether the changes in its size are related to a real increase in

size of both smallest and largest specimens, or to an increase in abundance of the largest morpho-species (Fig. 3).

5. Results

5.1. *Discorhabdus* abundances and accummulation rates

Nannofossil accummulation rates (NAR) of the total assemblage (coccoliths plus the nannolith *Schizosphaerella*) are the lowest in the Concavum zone, Late Aalenian ($0.187x10^9$ nannofossils$*m^{-2}*Ma^{-1}$), and the highest at the boundary of Sauzei/Humphresianum zones, Early Bajocian ($360x10^9$ nannofossils$*m^{-2}*Ma^{-1}$). In the same way, accumulation rates of *Discorhabdus* show a slight increase up-section. They vary between $0.016x10^9$ nannofossils $*m^{-2}*Ma^{-1}$ and $6x10^9$ nannofossils $*m^{-2}*Ma^{-1}$) from Concavum to Laeviscula zones, and $20x10^9$ nannofossils$*m^{-2}*Ma^{-1}$ and $80x10^9$ coccoliths$*m^{-2}*Ma^{-1}$ in the Sauzei zone (Fig. 3).

In the total nannofossils assemblage, *Discorhabdus* is frequent (~23%) to rare (~2%) in marlstones, and frequent (~18%) to absent in limestones. While *D. ignotus* and *D. striatus* are consistent along the interval studied, *D. criotus* is only recorded in samples CM12 and CM15 (Fig. 3).

The highest relative abundances of *D. ignotus* are recorded in the Concavum and Discites zones (around 15% and 18%, respectively), whereas they decrease from the end of the Discites zone to the Sauzei zone (1% - 5%). On the contrary, *D. striatus* displays lower relative abundances (~5%) within the Concavum Zone and progressively increases from the Discites zone upwards (Fig. 3).

5.2. Biometry

5.2.1. Statistical analysis

Mean, median, minimum and maximum values of the different measured parameters of *D. striatus*, *D. ignotus* and *D. criotus* are summarized in Table 1. On the basis of these results, *D. criotus* is in the same size range as *D. ignotus*, thus *D. striatus* can be discriminated with respect to the pool *D. ignotus*-*D. criotus*. On the other hand, central area seems to be smaller in size (L) in *D. ignotus* compared to *D. striatus* and *D. criotus*. Thus, proportions of the central area with respect to distal shield indicate that central area represents the half of the L axis of *D. criotus*., while it represents around the 40% of the L axis of *D. striatus* and *D. ignotus*. Coccolith ellipticity does not show strong differences between the three morphotypes as it was indicated by values between 0.96 and 1. However, this pool can result from a bias due to the extremely low proportion of *D. criotus* in the assemblage.

Table 2 shows significant positive correlations (0.825<r>0.981; $p < 0.0001$) between L axis and l axis of both proximal and distal shields and between L axis and central area. We only show in Table 2, L axis of distal shield because this is the most representative size descriptive parameter for *Discorhabdus*. The number of elements is less significantly correlated to size of distal or proximal shields (Table 2).

5.2.2. Biometric trends

The mean size of distal shield of *Discorhabdus* coccoliths increases from the Late Aalenian to the Early Bajocian (Figs. 3 and 5). Thus, smaller *Discorhabdus* characterize the interval comprised between the Concavum Zone and the earliest part of the Laeviscula Zone. While larger *Discorhabdus* characterize the Laeviscula and Sauzei Zones dated from the Bajocian. Additionally, both sizes of smaller and larger specimens increase up-section, as revealed by percentile results (Fig. 3).

5.2.3. Mixture analysis

Within the pool of *Discorhabdus* (*striatus* + *ignotus* + *criotus*), mixture analyses show a bimodal trend suggesting the existence of two group sizes with a boundary at 5 µm for the distal shield L axis, and at 4.3 µm for the proximal shield L axis (Fig. 4). Central area L axis reveals a unimodal distribution (Fig. 4).

6. Discussion

6.1. Biometric characterization of *Discorhabdus* pool

One of the major goals of this work is to assess an accurate taxonomic characterization of *Discorhabdus* in order to quantitatively describe the morpho-species. *Discorhabdus* coccoliths belong to the family Biscutaceae and first occur during the Early Jurassic (see compilation in Mattioli and Erba, 1999). They are common to abundant during the Jurassic and are well represented until Late Cretaceous (Watkins, 1989; Crux, 1991; Erba, 1991; Erba et al., 1992; Gale et al., 1996; Nederbragt and Fiorentino, 1999; Kennedy et al., 2000; Giraud et al., 2003; Herrle, 2003; Herrle and Mutterlose, 2003; Bornemann et al., 2005; Bown, 2005; Linnert et al., 2010; Herrle et al., 2010).

The original diagnosis of *Discorhabdus* provided by Noël (1965) was erected for circular placolith coccolith outlines that present two unicyclic shields. The distal shield is wider than the proximal one; both are formed by radial, non-imbricated calcite elements. The central area is formed by a depression that contains in its centre granular microcrystals, and a small perforation at the base of a tiny spine (not always preserved). All these diagnostic features described by Noël (1965) were also noted by other authors (Perch-Nielsen, 1968; Moshkovitz and Ehrlich, 1976; Perch-Nielsen, 1985; Bown, 1987a; Bown, 1987b; Bown et al., 1988, Reale et al., 1992; Cobianchi, 1992, Mattioli and Erba, 1999) and in this study.

Later, de Kaenel and Bergen (1993) emended the original diagnosis. These authors argued that *Discorhabdus* also comprises elliptical coccoliths, whose unicyclic shields are

constructed of non-imbricated to slightly overlapping radial elements. In addition, the structure of the central area is composed of several perforations near the base of the distal projection.

Circular shape of *Discorhabdus* has been well discussed and accepted by several authors (Perch-Nielsen, 1968; Moshkovitz and Ehrlich, 1976; Perch-Nielsen, 1985; Bown, 1987a, b; Bown et al., 1988, Reale et al., 1992; Cobianchi, 1992, Mattioli and Erba, 1999, Mattioli et al., 2004b). In this paper, *Discorhabdus* is taxonomically discriminated from *Biscutum* and *Similiscutum* by its circular morphology, where no imbrication occurs in the radial elements, by its conical and smaller central area that contains radial microcrystals and a central pore (when it is present), and its relative central area birefringence under LM.

Concerning the different morpho-species, according to Moshkovitz and Ehrlich (1976) and Perch-Nielsen (1968), *D. striatus* is characterized by relatively large forms, although some authors consider lower sizes of the total diameter as indicated in Table 3. *D. striatus* is also distinguished by a very small opening or closed central area, and a relatively high birefringence under polarized light. The number of radial elements sums 20 to 24, which are joined along radial sutures. *D. ignotus* is characterized by relatively smaller forms (Table 1) and a central depression, relatively wider than that of *D. striatus*. Dark grey colors and an open and highly birefringent central area are the major diagnostic features for *D. criotus* (Bown, 1987a; Fig. 2).

Mixture analysis of our dataset shows that there is a significant difference between a group of *Discorhabdus* smaller than 5 µm and a group larger than 5 µm. This observation and a higher birefringence observed in the larger group make us consider that the small group corresponds to *D. ignotus* and the larger group corresponds to *D. striatus*. Our quantitative data also indicate that neither the number of elements nor the size of the central area may differentiate the three morphotypes (Table 1). However, the proportion of the central area respect to the

distal shield may discriminate *D. ignotus* and *D. striatus* from *D. criotus*. Unfortunately, our biometric study does not allow us to better describe *D. criotus* because of the few number of specimens encountered in the studied section.

6.2. Paleoenvironmental/Paleoceanographic conditions and *Discorhabdus* size

Size pattern of *Discorhabdus* recognized from Late Aalenian to Early Bajocian (Figs. 3, 4 and 5) may represent a response to a paleoecological constraint (trophic conditions, temperature or salinity). We compare *Discorhabdus* size pattern to trophic levels as inferred on the basis of nannofossil accumulation rates and of bulk rock $\delta^{13}C$ measured in the Cabo Mondego section (Figs. 3 and 5). The *Discorhabdus* size increases along with nannofossil accumulation rates and $\delta^{13}C$. Some studies have shown that high accumulation rates of nannofossils can reflect an increase in productivity of surface waters in the Mesozoic (Mattioli and Pittet, 2002; Bornemann et al., 2003; Gréselle et al., 2011). In addition, a number of studies have illustrated that variations of $\delta^{13}C$ are linked to marine productivity. In fact, phytoplankton preferentially incorporates light C (^{12}C) during photosynthesis, so that carbonates precipitating in surface waters are enriched in ^{13}C (REFS). Thus, high $\delta^{13}C$ excursions represent intervals of high primary productivity (AUTHORS). In that way, the increase in nannofossil accumulation rates (Fig. 3) recorded in the Cabo Mondego section from the Laeviscula zone (Early Bajocian) upwards, suggests an increase in nannofossil productivity. Furthermore, a slight increase in $\delta^{13}C$ (Suchéras-Marx et al., 2011) is recorded in the Cabo Mondego section from the Late Aalenian to the Early Bajocian (Fig. 3). Other studies document a trend of $\delta^{13}C$ to more positive values in the Early Bajocian (Bartolini et al., 1996, 1999 in Colle Bertone and Monte Terminilleto sections, Central Italy), and Bartolini and Cecca (1999) in Umbria-Marche sections in Italy; O'Dogherty et al (2006), in Casa Blanca,

Agua Larga and Puerto Escaño sections; Sandoval et al (2008), in Agua Larga and Cerro de Mahoma sections in the Iberian paleomargin; Gómez et al (2009), in the Basque Cantabrian Basin; Brigaud et al (2009), in the Eastern Paris Basin; and Price (2010) in the Isle of Raasay (Fig. 5). These authors interpreted the carbon isotope trend as a gradual eutrophication of marine surface waters. Therefore, this association of events provides support that enhancing productivity in surface waters related to eutrophication from Late Aalenian to Early Bajocian is a supra-regional rather than a local event.

Parallel to the increase in both nannofossil accumulation rates and $\delta^{13}C$, a trend to higher relative abundance of *D. striatus* is also observed (Fig. 3). This dominance of *D. striatus* within the *Discorhabdus*'s pool largely contributes to the observed rise in size. Until now, nothing is known about the paleoecological preferences of *D. striatus*, but our results suggest that this morpho-species had probable affinities for high trophic levels.

Although this strong evidence for increasing nutrient levels in the course of the Early Bajocian, a link between sea-surface temperature and the increasing *Discorhabdus* size up-section cannot be excluded. Paleoclimate proxies have documented the evidence for a supra-regional change in sea temperature in adjacent Mediterranean-Tethys settings. According to the compilation of the $\delta^{18}O$ data (Fig. 5) from Paris Basin (Brigaud et al., 2009) and Basque-Cantabrian Basin (Gómez et al., 2009), an increase in the sea temperatures is recorded from Concavum (16-23°C) to Discites Zones (15°-25°C). Relatively steady temperatures occur from Discites to Laeviscula Zones, even if sample density is weaker in this interval. In the Sauzei Zone, a rise in temperature is observed spanning from 22° to 35°C. Although paleotemperature data are not available in the Lusitanian Basin for this time interval, the effects of a supra-regional sea temperature rise on the *Discorhabdus* size increase may not be discarded.

Salinity is also a parameter that can control species size of modern and culture coccoliths (Green et al., 1998; Bollmann and Herrle, 2007). Variations in sea surface salinity can be triggered by enhanced river discharge. However, sedimentological, geochemical and micropaleontological data attesting for increased river discharge in the Lusitanian Basin are not available.

6.3. Changes in *Discorhabdus* size: an evolutionary process?

Our results also call into question the existence of a biological evolutionary cause that would explain the increase trend in *Discorhabdus* size from Late Aalenian to Early Bajocian. This general trend seems to outstandingly follow the history of radiation and increase of abundances of calcareous nannofossils during Middle Jurassic (see the introductory paragraph). This hypothesis points to the size spectra of *Discorhabdus* up-section is correlative and strongly influenced by the calcareous nannofossil turnover event occurring at the Aalenian/Bajocian boundary. An apparently general feature in calcareous nannofossil taxa is the tendency for species size to increase over Mesozoic (from Sinemurian to Santonian) being associated to radiation or increase in diversity (Bown et al., 2004). Such trend has been particularly remarked over Early Jurassic (associated to the Early Jurassic radiation; Bown et al., 2004) and Jurassic/Cretaceous turnover (in agreement with maximum diversity; Aubry et al., 2005). However, the existence of a decrease size gradient during Early Toarcian (Mattioli et al., 2004b; Fraguas and Young, 2011), mid-Campanian (Aubry et al., 2005) and Maastrichtian (Bown et al., 2004) was also detected, but it equally parallels a decrease in diversity probably reflecting an important perturbation in the global climatic system (Aubry et al, 2005). Such a size trend of *Discorhabdus* is an illustration of Cope's rule, who stated that population lineages tend to increase in size over evolutionary time (Hone and Benton, 2005). In this regard, definition of Cope's rule by Ghiselin (1972) strictly affirmed that "evolution

proceeds in the direction of increasing body size"; and Trammer (2002, 2005) established that Cope's rule is "an increase in maximum body size during evolutionary radiation of a clade".

Although paleoecological constraints exert an important influence on the *Discorhabdus* size pattern, the evolutionary hypothesis appears not negligible. In summary, the existence of significant correlations between paleoecological constraints and an evolutionary factor in *Discorhabdus*'s pool supports the importance of those issues as determinants on its body size and abundance.

7. Summary and Conclusions

Mixture analyses applied to a dataset of 29 samples and 984 specimens display a bimodal frequency distribution in the *Discorhabdus* size in the Cabo Mondego section. The consistent bimodal pattern supports that 5 μm can be considered as the coccolith size boundary for distal shield. In the literature, only size ranges are reported for *Discorhabdus* (or *Tremalithus* or *Bidiscus*) *ignotus* and *Discorhabdus striatus* (and *Discorhabdus* aff. *D. striatus*). These are comprised, respectively, between 2.3 μm and 6.40 μm, and between 5 μm and 8 μm (Table 3). Thus, our statistical analyses contribute to improve taxonomic characterization.

Discorhabdus size increases from the Late Aalenian to the Early Bajocian. This rise represents both an increase in the abundance of *D. striatus* (the largest species) and an increase in size of the whole *Discorhabdus*'s pool.

Discorhabdus size is associated to an increase in the absolute *Discorhabdus* abundance, a rise in the total nannofossil accumulation rates and slight increasing values of $\delta^{13}C$ of Cabo Mondego section and adjacent Mediterranean-Tethys settings. This scenario may suggest that the increasing trends in *D. striatus* abundance and in size of the total *Discorhabdus*'s pool are due to a rise in nutrient concentration in the sea-surface waters as the result of a gradual eutrophication.

Compilation of previous reconstructions of $\delta^{18}O$ data of Tethyan settings has demonstrated a gradual increase of sea temperatures in adjacent Mediterranean Tethys. Although information of the gradual advection of relatively warmer water masses in Cabo Mondego section is not still presented, the effect of a supra-regional sea temperature rising on the *Discorhabdus* size up-section may not be discarded.

A parallel increase in size of *Discorhabdus* during times of calcareous nannofossil turnover during Late Aalenian to Early Bajocian illustrates the Cope's rule. This implies that an increase of maximum size of those coccoliths occurred during times of enhanced radiation and abundances of calcareous nannofossils over Middle Jurassic.

In synthesis, both environmental and evolutionary parameters may control the trend in *Discorhabdus* size observed in the Cabo Mondego section. Further studies are needed to better constrain which of these parameters is dominant.

Acknowledgements

This study was supported by the projects BQR of the Université Lyon 1 2006 to FG, BQR 2010 and INSU 2011 Syster/Interrvie to EM. The Laboratory UMR 5276 of the University Lyon 1 is also acknowledged. This study was supported by a post-doctoral grant of the CNRS/INSU (Centre National de la Recherche Scientifique/Institut National des Sciences de l'Univers) to G.E. López-Otálvaro. This manuscript was highly improved by the suggestions and comments of XXXXXX.

9. Appendix A: Taxonomy

9.1. Systematic paleontology

Division **Haptophyta** Hibberd, 1972

Class **Prymnesiophyceae** Hibberd, 1976

Order **Coccolithales** Schwarz, 1932

Family **Biscutaceae** Black, 1971 emend. Bown, 1987

Genus ***Discorhabdus*** Noël, 1965

Type species: *Discorhabdus patulus* (Deflandre, 1954) Noël, 1965

Diagnosis: "Circular base composed of two superimposed simple shields, joined firmly, perforated in the centre to allow the passage of a variably developed spine. The distal shield is constructed from a single series of calcite lamellae which are radially disposed, joined all along their length giving the disc a continuous surface, without festoons. The proximal disc, generally smaller than or equal to the distal disc is formed form the same number of calcite plates, flat, often thinner, similarly joined and radially disposed. This proximal disc, slightly convex, forms a solid base pierced only at its centre by the root of the spine. The axial spine with a variable diameter and of variable length and morphology is made up of crystals of calcite, almost cubic, or elongate rhombohedra, arranged about a central canal. The outer edge of the spine is closely coupled to the inner edge of the perforations of the distal and proximal disc" (Noël 1965, p. 138).

Discorhabdus ignotus (Górka, 1957) Perch-Nielsen, 1968

1957 *Tremalithus ignotus* Górka, pp. 248, 272, fig. 9

1968 *Discorhabdus ignotus* (Górka); Perch-Nielsen, p. 81, text-fig. 41; pl. 28, fig. 6

1969 *Striatococcus nebulosus* Prins, pl. 2, fig. 16 (*nom. nud.)*

1971 *Discorhabdus* sp.; Rood et al., p. 279, pl. 4, fig. 8.

1975 *Bidiscus ignotus* (Górka) Hoffmann, 1970; Grün and Allemann, p. 157, text-fig. 4; pl. 1, figs. 8-10

1977 *Discorhabdus ignotus* (Górka, 1957) Perch-Nielsen, 1968; Hamilton, p. 592, pl. 2, figs. 1-11; p. 596, pl. 4, fig. 10 top.

non 1977 *Discorhabdus ignotus* (Górka, 1957) Perch-Nielsen, 1968; Hamilton, pl. 2, fig. 2

non 1977 *Discorhabdus ignotus* (Górka, 1957) Perch-Nielsen, 1968; Hamilton, p. 592, pl. 2, figs. 1-11; p. 596, pl. 4, figs. 10 (bottom), 11.

1979 *Discorhabdus ignotus* (Górka, 1957) Perch-Nielsen, 1968; Hamilton, p. 17, pl. figs. 10-11 (non fig. 9).

1979 *Discorhabdus* sp. 2; Medd, p. 101, pl. 7, figs. 8.

1984 *Discorhabdus superbus* (Deflandre, 1954); Crux, fig. 9 (7-8)

1986 *Discorhabdus ignotus* (Górka, 1957) Perch-Nielsen, 1968; de Wever et al., p. 183, pl. 13, fig. 4.

1986 *Discorhabdus ignotus* (Górka, 1957) Perch-Nielsen, 1968; Manivit et al., p. 122, pl. 3, fig. 4.

1987b *Discorhabdus ignotus* (Górka, 1957) Perch-Nielsen, 1968; Bown, p. 51, pl. 7, fig. 1 (non figs. 2, 3).

1986 *Discorhabdus* sp.; Young et al., pl. 1, fig. E

1987 *Discorhabdus superbus* (Deflandre); Crux, pl. 1, figs. 8-10

non 1987b *Discorhabdus ignotus* (Gorka, 1957) Perch-Nielsen, 1968; Bown (partim), p. 51; pl. 7, figs. 2-3; p. 79, pl. 14, figs. 7-8.

1990 *Discorhabdus ignotus* (Górka, 1957) Perch-Nielsen, 1968; Baldanza et al., p. 233, fig. 2.

1990 *Biscutum dubium* (Noël, 1965), Grün et al. 1974; Baldanza et al., p. 233, fig. 1.

1991 *Discorhabdus ignotus* (Górka, 1957) Perch-Nielsen, 1968; Baldanza and Mattioli, p. 141, pl. 2, fig. 19.

1991 *Discorhabdus ignotus* (Górka, 1957) Perch-Nielsen, 1968; Reale et al., p. 71, pl. 1, figs. 17-20; p. 73, pl. 2, figs. 1, 4, 5, 6 (non figs. 2-3).

1991 *Discorhabdus striatus* Moshkovitz and Erlich, 1976; Reale et al., p. 73, figs. 7-9.

1992 *Discorhabdus striatus* Moshkovitz and Erlich, 1976; Cobianchi, p. 97, fig. 20a.

1994 *Discorhabdus ignotus* (Górka, 1957) Perch-Nielsen, 1968; Bucefalo Palliani and Mattioli, p. 140, pl. 1, figs. 3, 6.

1994 *Discorhabdus ignotus* (Górka, 1957) Perch-Nielsen, 1968; Gardin and Manivit, p. 233, pl. 2, figs. 9-10.

1994 *Discorhabdus ignotus* (Górka, 1957) Perch-Nielsen, 1968; Galbrun et al., p. 585, pl. 3, figs. 5-6.

1994 *Discorhabdus ignotus* (Górka, 1957) Perch-Nielsen, 1968; Goy et al., p. 29, pl. 6, figs. 9, 13.

1996 *Discorhabdus striatus* Moshkovitz and Erlich, 1976; Baldanza et al., p. 32, fig. 11.

1996 *Discorhabdus striatus* Moshkovitz and Erlich, 1976; Picotti and Cobianchi, p. 218, fig. 15.

1996 *Discorhabdus* sp.; Picotti and Cobianchi, p. 218, fig. 16.

1999 *Discorhabdus ignotus* (Górka, 1957) Perch-Nielsen, 1968; Aguado et al., p. 13; pl. 8, fig. 38.

1999 *Discorhabdus ignotus* (Górka, 1957) Perch-Nielsen, 1968; Mattioli and Erba, p. 367; pl. 2, figs. 17-18.

2000 *Discorhabdus ignotus* (Górka, 1957) Perch-Nielsen, 1968; Kennedy et al, p. 646; pl. 33 (upper left), fig. k.

2003 *Discorhabdus ignotus* (Górka, 1957) Perch-Nielsen, 1968; Bornemann et al., p. 198; pl. 5, fig. 8.

2005 *Discorhabdus ignotus* (Górka, 1957) Perch-Nielsen, 1968; Bown, p. 71, pl. 7, fig. 4.

2005 *Discorhabdus ignotus* (Górka, 1957) Perch-Nielsen, 1968; Lees and Bown, p. 47, fig. 10, 11.

2006 *Discorhabdus ignotus* (Górka, 1957) Perch-Nielsen, 1968; Mailliot et al., p. 567, pl. 1.

2006 *Discorhabdus striatus* Moshkovitz and Erlich, 1976; Mailliot et al., p. 567, pl. 1.

2010 *Discorhabdus ignotus* (Górka, 1957) Perch-Nielsen, 1968; Linnert et al., p. 41; pl. 1, fig. 17.

2011 *Discorhabdus ignotus* (Górka, 1957) Perch-Nielsen, 1968; Linnert et al., p. 511; pl. 1, fig. 15.

Diagnosis: Gorka (1957) did not provide a diagnosis.

L.M. description: Circular placolith smaller than 5 µm, composed of two shields (proximal and distal). Twenty or twenty-two radial, non-imbricated and easily distinguished elements are arranged in both shields. Central area is illustrated by a central depression, a pore than may be open or closed and a tiny spine that may be present. The placoliths are characterized by a moderate birefringence.

Dimensions: Distal shield L axes: 2.42-4.92 µm; proximal shield L axes: 2.08-4.50 µm; central area L axes: 0.83-2.58 µm.

Discorhabdus striatus Moshkovitz and Ehrlich, 1976

1969 *Striatococcus nebulosus* Prins, pl. 2, fig. 16 (*nom. nud.*)

1976 *Discorhabdus striatus* Moshkovithz and Ehrlich, p. 14; pl. 7, figs. 1-5.

1977 *Discorhabdus ignotus* (Górka, 1957) Perch-Nielsen, 1968; Hamilton, p. 592, pl. 2, figs. 1-11; p. 596, pl. 4, figs. 10 (bottom), 11.

1979 *Discorhabdus ignotus* (Górka, 1957) Perch-Nielsen, 1968; Hamilton, p. 17, pl. fig. 9.

1987b *Discorhabdus ignotus* (Gorka, 1957) Perch-Nielsen, 1968; Bown (partim), p. 51; pl. 7, figs. 2-3; p. 79, pl. 14, figs. 7-8.

1988 *Discorhabdus striatus* Moshkovitz and Ehrlich, 1976; Bown, Cooper and Lord, p. 113; pl. 1, figs. 17-18

1991 *Discorhabdus ignotus* (Górka, 1957) Perch-Nielsen, 1968; Reale et al., p. 73, pl. 2, figs. 2-3.

1991 *Discorhabdus striatus* Moshkovitz and Ehrlich, 1976; Reale et al., p. 73, pl. 2, figs. 10-12 (non figs. 7-9).

non 1991 *Discorhabdus striatus* Moshkovitz and Ehrlich, 1976; Reale et al., p. 73, figs. 7-9.

non 1992 *Discorhabdus striatus* Moshkovitz and Ehrlich, 1976; Cobianchi, p. 97, fig. 20a.

1992 *Discorhabdus* aff. *D. striatus* Moshkovitz and Ehrlich, 1976; Cobianchi, p. 97, figs. 20b-d.

1993 *Biscutum striatum* Moshkovitz and Ehrlich, 1976; de Kaenel and Bergen, pl. 3, fig. 8

1994 *Discorhabdus striatus* Moshkovitz and Ehrlich, 1976; Goy et al., p. 29, pl. 6, figs. 10, 14.

1994 *Biscutum* cf. *novum* (Goy, 1979) Bown 1987; Goy et al., p. 29, pl. 6, figs. 11, 12, 16.

1995 *Discorhabdus striatus* Moshkovitz and Ehrlich, 1976; Stoico and Baldanza, p. 109, pl. 5, fig. 10.

non 1996 *Discorhabdus striatus* Moshkovitz and Ehrlich, 1976; Baldanza et al., p. 32, fig. 11.

non 1996 *Discorhabdus striatus* Moshkovitz and Ehrlich, 1976; Picotti and Cobianchi, p. 218, fig. 15.

1998 *Discorhabdus striatus* Moshkovitz and Ehrlich, 1976; Parisi et al., p. 31; pl. 5, figs. 2, 5.

1999 *Discorhabdus striatus* Moshkovitz and Ehrlich, 1976; Mattioli and Erba, p. 367; pl. 2, figs. 16, 19, 20.

non 2006 *Discorhabdus striatus* Moshkovitz and Ehrlich, 1976; Mailliot et al., p. 567, pl. 1.

2006 *Discorhabdus striatus* Moshkovitz and Ehrlich, 1976; Perilli and Duarte, p. 431, pl. 1., figs. 11, 13.

2009 *Discorhabdus striatus* Moshkovitz and Ehrlich, 1976; Giraud et al., p. 133, fig. 4.7.

2009 *Discorhabdus striatus* Moshkovitz and Ehrlich, 1976; Giraud, p. 703, fig. 3.6.

Diagnosis: Moshkovitz and Ehrlich (1976) did not provide a diagnosis.

L.M. description: Circular placolith larger than 5 µm, composed of two shields (proximal and distal). Twenty four radial, non-imbricated and easily distinguished elements are arranged in both shields. Central area is occupied by a central depression, a pore than may usually be closed and a tiny spine that may be present. The placoliths are characterized by a high birefringence.

Dimensions: Distal shield L axes: 5-8.58 µm; proximal shield L axes: 3.83-7.25 µm; central area L axes: 1.50-3.75 µm.

Discorhabdus criotus Bown, 1987

1969 *Palaeopontosphaera repleta* Prins, pl. 2, fig. 11 (*nom. nud*.)

1977 *Discorhabdus ignotus* (Górka, 1957) Perch-Nielsen, 1968; Hamilton, pl. 2, fig. 2

1994 *Discorhabdus criotus* (Górka, 1957) Perch-Nielsen, 1968; Gardin and Manivit, p. 233, pl. 2, figs. 11-12.

1996 *Discorhabdus criotus* Bown, 1987; Baldanza et al., p. 32, fig. 10.

1998 *Discorhabdus criotus* Bown, 1987; Parisi et al., p. 31; pl. 5, fig. 1.

1999 *Discorhabdus criotus* Bown, 1987; Mattioli and Erba, p. 367; pl. 3, figs. 1-3.

2006 Discorhabdus criotus Bown, 1987; Perilli and Duarte, p. 431, pl. 1, figs. 12, 14.

2006 *Discorhabdus criotus* Bown, 1987; Mailliot et al., p. 567, pl. 1.

Diagnosis: "A species of *Discorhabdus* with a small, distal inner cycle set deep in the central depression, and radiating sutures which bend in a counter-clockwise direction near the outer edge of the shield; no spine is present and the central area is a small circular pore". (Bown, 1987a, p. 49).

L.M. description: Circular placolith composed of two shields (proximal and distal). Twenty radial, non-imbricated and easily distinguished elements are arranged in both shields. Central

area is occupied by a central depression and an open pore. Central area is strongly birefringent with respect to the rest of the placolith.

Dimensions: Distal shield L axes: 4.75-4.92 µm; proximal shield L axes: 3.92-4.33 µm; central area L axes: 2.42-2.50 µm.

10. References

Aguado, R., O'Dogherty, L., Sandoval, J., 2008. Fertility changes in surface waters during the Aalenian (mid-Jurassic) of the Western Tethys as revealed by calcareous nannofossils and carbon-cycle perturbations. Marine Micropaleontology 68, 268-285.

Aubry, M.P., Bord, D., Beaufort, L., Kahn, A., Boyd, S., 2005. Trends in size changes in the coccolithophorids, calcareous nannoplankton, during the Mesozoic: A pilot study. Micropaleontology 51, 309-318.

Azerêdo, A.C., 1993. Jurássico Médio do Maciço Calcário Estremenho (Bacia Lusitânica): análise de fácies, micropaleontología, paleogeografía. Unpublished PhD Thesis. Departamento de Geologia da Faculdade de Ciências de Lisboa. 366p.

Azerêdo, A.C., 1998. Geometry and facies dynamics of Middle Jurassic carbonate ramp sandbodies , west-central Portugal. In: Wright, V.P., Burchette, T. (Eds.). Carbonate ramps. Geological Society of London Special Publications 149, 281-314.

Azerêdo, A.C., Ramalho, M.M., Wright, V.P., 1988. The Middle-Upper Jurassic disconformity in the Lusitanian Basin, Portugal: preliminary facies analysis and evidence for palaeoclimatic fluctuation. Cuadernos de Geología Ibérica 24, 99-119.

Bartolini, A., Cecca, F., 1999. 20 My hiatus in the Jurassic of Umbria-Marche Apennines (Italy): carbonate crisis due to eutrophication. Comptes Rendus de l'Académie des Sciences, Serie II. Sciences de la Terre et des Planètes 329, 587-595.

Bartolini, A., Baumgartner, P.O., Hunzinker, J., 1996. Middle and Upper Jurassic carbon stable-isotope stratigraphy and radiolarite sedimentation of the Umbria-Marche basin (Central Italy). Eclogae Geologicae Helvetiae 89, 811-844.

Bartolini, A., Baumgartner, P.O., Guex, J., 1999. Middle and Late Jurassic radiolarian palaeoecology versus carbon-isotope stratigraphy. Palaeogeography, Palaeoclimatology, Palaeoecology 145, 43-60.

Beaufort, L., 1991. Adaptation of the random settling method for quantitative studies of calcareous nannofossils. Micropaleontology 37, 415-418.

Bill, M., O'Dogherty, L., Guex, J., Baumgartner, P.O., Masson, H., 2001. Radiolarite ages in Alpine-Mediterranean ophiolites; constraints on the oceanic spreading and the Tethys-Atlantic connection. Geological Society of America Bulletin 113, 129-143.

Bollmann, J., 1997. Morphology and biogeography of *Gephyrocapsa* coccoliths in Holocene sediments. Marine Micropaleontology 29, 319-351.

Bollmann, J., Herrle, J.O., 2007. Morphological variation of *Emiliania huxleyi* and sea surface salinity. Earth and Planetary Science Letters 255, 273-288.

Bornemann, A., Mutterlose, J., 2006. Size analyses of the coccolith species Biscutum constans and Watznaueria barnesiae from the late Albian "Niveau Breistroffer" (SE France); taxonomic and palaeoecological implications. Geobios 39, 599-615.

Bornemann, A., Aschwer, U., Mutterlose, J., 2003. The impact of calcareous nannofossils on the pelagic carbonate accumulation across the Jurassic-Cretaceous boundary. Palaeogeography, Palaeoclimatology, Palaeoecology 199, 187-228.

Bornemann, A., Pross, J., Reichelt, K., Herrle, J.O., Hemleben, C., Mutterlose, J., 2005. Reconstruction of short-term palaeoceanographic changes during the formation of the Late Albian "Niveau Breistroffer" (OAD 1d, SE France). Journal of the Geological Society 162, 623-639.

Bown, P.R. 1987a. Taxonomy, evolution and biostratigraphy of Late Triassic-Early Jurassic calcareous nannofossils. The Paleontological Association. Special papers in Paleontology 38, 118p.

Bown, P.R. 1987b. The structural development of early Mesozoic coccoliths and its evolutionary and taxonomic significance. Abhandlungen der Geologischen Bundesanstalt 39, 33-49. Wien.

Bown, P.R., 2005. Early to mid-Cretaceous calcareous nannoplankton from the northwest Pacific Ocean, Leg 198, Shatsky Rise. In: Bralower, T.J., Premoli Silva, I., Malone, M.J. (Eds.), Proceedings ODP, Scientific Results, 198. Ocean Drilling Program, College Station, TX, pp. 1-82.

Bown, P.R., Cooper, M.K.E., 1998. Jurassic. In: Bown, P.R. (Ed.), Calcareous nannofossil biostratigraphy. British Micropaleontological Society Publications Series. Cambridge, pp.34-85.

Bown, P.R., Cooper, M.K.E., Lord, A.R. 1988. A calcareous nannofossil biozonation scheme for the early to mid Mesozoic. Newsletters on Stratigraphy 20, 91-114.

Bown, P.R., Lees, J.A., Young, J.R., 2004. Calcareous nannoplankton evolution and diversity through time. In: Thierstein, H.R., Young, J. (Eds.), Coccolithophores – From Molecular Processes to Global Impact. Springer, Berlin, pp. 481-508.

Brigaud, B., Durlet, C., Deconinck, J.-F., Vincent, B., Pucéat, E., Thierry, J., Trouiller, A., 2009. Facies and climate/environmental changes recorded on a carbonate ramp: A sedimentological and geochemical approach on Middle Jurassic carbonates (Paris Basin, France). Sedimentary Geology 222, 181-206.

Canales, M.L., Henriques, M.H., 2008. Foraminifera from the Aalenian and the Bajocian GSSP (Middle Jurassic) of Murtinheira section (Cabo Mondego, West Portugal):

Biostratigraphy and paleoenvironmental implications. Marine Micropaleontology 67, 155-179.

Cobianchi, M., 1992. Sinemurian-Early Bajocian calcareous nannofossil biostratigraphy of the Lombardy Basin (Southern Calcareous Alps, Northern Italy). Atti Ticinensi di Scienze della Terra 35, 61-106.

Cobianchi, M., Erba, E., Pirini Radrizzani, C., 1992. Evolutionary trends of calcareous nannofossil genera Lotharingius and Watznaueria during the Early and Middle Jurassic. Memorie di Scienze Geologiche XLIII, 19-25.

Coccioni, R., Erba, E., Premoli-Silva, I., 1992. Barremian-Aptian calcareous plankton biostratigraphy from the Gorgo Cerbara section (Marche, central Italy) and implications for plankton evolution. Cretaceous Research 13, 517-537.

Cresta, S., Pavia, G., 1994. Proceedings of the third international meeting on Aalenian and Bajocian stratigraphy: Miscellanea del Servizio Geologico d'Italia 5, 1-321

Crux, J.A., 1991. Calcareous nannofossils recovered by Leg 114 in the subantarctic South Atlantic Ocean. In: Ciesielski, P.F., Kristoffersen, Y., et al., (Eds.). Proceedings ODP, Scientific Results, 114. Ocean Drilling Program, College Station, TX, pp. 155–177. doi:10.2973/odp.proc.sr.114.123.1991

Erba, E., 1991. Calcareous nannofossil distribution in pelagic rhytmic sediments (Aptian-Albian Piobbico core, Central Italy). Rivista Italiana di Paleontologia e Stratigrafia 97, 455-484.

Erba E, Castradori D, Guasti G, Ripepe M., 1992. Calcareous nannofossils and Milankovitch cycles; the example of the Albian Gault Clay Formation (southern England). Palaeogeography Palaeoclimatology Palaeoecology 93, 47–69.

Erba, E., Bottini, C., Weissert, H.J., Keller, C.E., 2010. Calcareous nannoplankton response to surface-water acidification around oceanic anoxic event 1a. Science 329, 428-432.

Fraguas, A., Erba, E., 2010. Biometric analyses as a tool for the differentiation of two coccolith species of the genus *Crepidolithus* (Pliensbachian, Lower Jurassic) in the Basque-Cantabrian Basin (Northern Spain). Marine Micropaleontology 77, 125-136.

Fraguas, A., Young, J., 2011. Evolution of the coccolith genus *Lotharingus* during the Late Pliensbachian-Early Toarcian interval in Asturias (N Spain). Consequences of the Early Toarcian environmental perturbations. Geobios, *in press.*

Gale, A.S., Kennedy, W.J., Burnett, J.A., Caron, M., Kidd, B.E., 1996. The Late Albian to Early Cenomanian succession at Mont Risou near Rosans (Drôme, SE France): an integrated study (ammonites, inoceramids, planktonic foraminifera, nannofossils, oxygen and carbon isotopes). Cretaceous Research 17, 515-606.

Gardin, S., Manivit, H., 1991. Biostratigraphie des nannofossies calcaires du Toarcien du Quercy (sud-ouest de la France); comparison avec la coupe stratotypique de la cimenterie d'Airvault (Deux-Sevre, France). Geobios 17, 229-244.

Geisen, M., Bollmann, J., Herrle, J.O., Mutterlose, J., Young, J., 1999. Calibration of the random settling technique for calculation of absolute abundances of calcareous nannofossils. Micropaleontology 45, 437-442.

Ghiselin, M.T., 1972. Models in phylogeny. In: Schopf, T.J.M. (Eds.). Models in Paleobiology. Freeman, Cooper & Company, San Francisco, pp. 130-145.

Giraud, F., 2009. Calcareous nannofossil productivity and carbonate production across the Middle-Late Jurassic transition in the French Subalpine Basin. Geobios 42, 699-714.

Giraud, F., Olivero, D., Baudin, F., Reboulet, S., Pittet, B., Proux, O., 2003. Minor changes in surface-water fertility across the oceanic anoxic event 1d (latest Albian, SE France) evidenced by calcareous nannofossils. International Journal of Earth Sciences 92, 267–284.

Giraud, F., Pittet, B., Mattioli, E., Audouin, V., 2006. Paleoenvironmental controls on the morphology and abundance of the coccolith *Watznaueria britannica* (Late Jurassic, southern Germany). Marine Micropaleontology 60, 205-225.

Giraud, F., Courtinat, B., Atrops, F., 2009. Spatial distribution patterns of calcareous nannofossils across the Callovian-Oxfordian transition in the French Subalpine Basin. Marine Micropaleontology 72, 129-145.

Gómez, J.J., Canales, M.L., Ureta, S., Goy, A., 2009. Palaeoclimatic and biotic changes Turing the Aalenian (Middle Jurassic) at the southern Laurasian Seaway (Basque-Cantabrian Basin, northern Spain). Palaeogeography, Palaeoclimatology, Palaeoecology 275, 14-27.

Gorka, H., 1957. Coccolithophoridae z Gornego Mastrychtu Polski Srodkowej. Acta Palaeontologica Polonica 2, 235-284.

Gradstein, F.M., Ogg, J.G., Smith, A.G., Bleeker, W., Lourens, L.J., 2004. A new geologic Time Scale, with special reference to Precambrian and Neogene. Episodes 7, 83-100.

Green, J.C., Heimdal, B.R., Paasche, E., Moate, R., 1998. Changes in calcification and the dimensions of coccoliths of *Emiliania huxleyi* (Haptophyta) grown at reduced salinities. Phicologia 37, 121-131.

Gréselle, B., Pittet, B., Mattioli, E., Joachimski, M., Barbarin, N., Riquier, L., Reboulet, S., Pucéat, E., 2011. The Valanginian isotope event: A complex suite of palaeoenvironmental perturbations. Palaeogeography, Palaeoclimatology, Palaeocology 306, 41-57.

Grün, W., Alleman, F., 1975. The Lower Cretaceous of Caravaca (Spain): Berriasian calcareous nannoplankton of the Miravetes section (Subbetic Zone, Prov. of Murcia). Eclogae Geologicae Helvetiae 68, 147-211.

Hammer, Ø., Harper, D.A.T., Ryan, P.D., 2001. PAST : Paleontological statistics software package for education and data analysis. Palaeontologia Electronica 4, 1-9.

Hamilton, G., 1977. Early Jurassic calcareous nannofossils from Portugal and their biostratigraphic use. Eclogae Geologicae Helvetiae 70, 575-597.

Hamilton, G., 1979. Lower and Middle Jurassic calcareous nannofossils from Portugal. Eclogae Geologicae Helvetiae 72, 1-17.

Harper, D.A.T., 1999. Numerical paleobiology. John Wiley & Sons, Chichester. pp.

Henderiks. J., Pagani, M., 2007. Coccolithophore cell size and the Paleogene decline in atmospheric CO_2. Earth Planetary Science Letters 269, 576-584.

Henriques, M.H., Gardin, S., Gomes, C.R., Soares, A.F., Rocha, R.B., Marques, J.F., Lapa, M.R., Montenegro, J.D., 1994. The Aalenian-Bajocian boundary at Cabo Mondego (Portugal). In: Cresta, S., Pavia, G. (Eds.). Third International Meeting on Aalenian and Bajocian Stratigraphy. Miscellanea del Servizio Geologico Nazionale 5, 63-77.

Herrle, J.O., 2003. Reconstructing nutricline dynamics of mid-Cretaceous oceans: evidence from calcareous nannofossils from the Niveau Paquier black shale (SE France). Marine Micropaleontology 47, 307–321.

Herrle, J.O., Mutterlose, J., 2003. Calcareous nannofossils from the Aptian-Lower Albian of southeast France: palaeoecological and biostratigraphic implications. Cretaceous Research 24, 1-22.

Herrle, J.O., Pross, J., Friedrich, O., Kôβler, P., Hemleben, C., 2003. Forcing mechanisms for mid-Cretaceous black shale formation: evidence from the Upper Aptian and Lower Albian of the Vocontian Basin (SE France). Palaeogeography, Palaeoclimatology, Palaeoecology 190, 399-426.

Herrle, J.O., Kössler, P., Bollmann, J., 2010. Palaeoceanographic differences of early Late Aptian black shale events in the Vocontian Basin (SE France), Palaeogeography, Palaeoclimatology, Palaeoecology 297, 367-376.

Hesselbo, S.P., Jenkyns, H.C., Duarte, V., Oliveira, L.C.V., 2003. Carbon-isotope record of the Early Jurassic (Toarcian) Oceanic Anoxic Event from fossil wood and marine carbonate (Lusitanian Basin, Portugal). Earth Planetary Science Letters 253, 455-470.

Hone, D.W.E., Benton, M.J., 2005. The evolution of large size: how does Cope's Rule work? Trends in Ecology and Evolution 20, 4-6.

de Kaenel, E., Bergen, J.A., 1993. New Early and Middle Jurassic coccolith taxa and biostratigraphy from the Eastern proto-Atlantic (Morocco, Portugal and DSDP Site 547 B). Eclogae Geologicae Helvetiae 86, 861-907.

Keupp, H., 1976. Kalkiges Nannoplankton aus den Solnhofener Schichten (Unter-Tithon, Südliche Frankenalb). Neuess Jahrbuch für Geologie und Paläontologie 6, 361-381.

Keupp, H., 1977. Ultrafazies et genese der Solnhofener Plattenkalk (Oberer Malm, Sûdlichen Frankenalb). Abhandlungen der Naturhistorischen Gesellchaft zu Nürnberg 37, 128p.

Kennedy W. J., Gale A. S., Bown P. R., Caron M., Davey R. J., Gröcke D. and Wray D. S., 2000. Integrated stratigraphy across the Aptian-Albian boundary in the Marnes Bleues, at the Col de Pré-Guittard, Arnayon (Drôme), and at Tartonne (Alpes-de-Haute-Provence), France: a candidate Global Boundary Stratotype Section and Boundary Point for the base of the Albian Stage. Cretaceous Research 21, 591–720.

Linnert, C., Mutterlose J., Erbacher J., 2010. Calcareous nannofossils of the Cenomanian/Turonian boundary interval from the Boreal Realm (Wunstorf, northwest Germany) Marine Micropaleontology 74, 38–58.

Mattioli, E., Erba, E., 1999. Biostratigraphic synthesis of calcareous nannofossils events in the Tethyan Jurassic. Rivista Italiana di Paleontologia e Stratigrafia 105, 343-376.

Mattioli. E., Pittet, B., 2002. The contribution of calcareous nannoplankton to the carbonate deposition: a new approach applied to the Lower Jurassic of central Italy. Marine Micropaleontology 45, 175-190.

Mattioli, E., Pittet, B., Bucefalo Palliani, R., Röhl, H.J., Schmid-Röhl, A., Morettini, E., 2004a. Phytoplancton evidence for the timing and correlation of palaeoceanographical changes during the early Toarcian oceanic anoxic event (Early Jurassic). Journal of the Geological Society of London 161, 686-693.

Mattioli. E., Pittet, B., Young, J., Bown, P., 2004b. Biometric analysis of Pliensbachian-Toarcian (Lower Jurassic) coccoliths of the family Biscutaceae: intra- and interspecific variability versus palaeonvironmental influence. Marine Micropaleontology 52, 5-27.

Mattioli, E., Pittet, B., Suan, G., Maillot, S., 2008. Calcareous nannoplankton changes across the early Toarcian oceanic event in the western Tethys. Paleoceanography 23. doi:10.1029/2007PA001435.

Morettini, E., Santantonio, M., Bartolini, A., Cecca, F., Baumgartner, P.O., Hunziker, J.C., 2002. Carbon isotope stratigraphy and carbonate production during the Early-Middle Jurassic: examples from the Umbria-Marche-Sabina Apennines (central Italy). Palaeogeography, Palaeoclimatology, Palaeoecology 184, 251-273.

Morris, P.H., 1982. Distribution and palaeoecology of Middle Jurassic foraminifera from the Lower Inferior Oolite of the Cotswolds. Palaeogeography, Palaeoclimatology, Palaeoecology 37, 319-347.

Morris, P.H., Coleman, B.E., 1989. The Aalenian to Callovian. In: Jenkins, D.G., Murray, J.W. (Eds.). Stratigraphical Atlas of Fossil Foraminifera. Second Edition, Ellis Horwood Ltd., Chichester, England, 189-236.

Moshkovitz, S., Ehrlich, A., 1976. Distribution of Middle and Upper Jurassic calcareous nannofossils in the Northeastern Negev, Israel and in Gebel Maghara, Northern Sinai. Bulletin of the Geological Survey of Israel 69, 1-42.

Mougenot, D., Monteiro, J.H., Dupeuble, P.A., Malod, J.A., 1979. La marge continentale sud-portugaise; évolution structurale et sédimentaire. Ciencias da Terra 5, 223-245.

Mouterde, R., Ramalho, M., Rocha, R.B., Ruget, C., Tintant, H., 1971. Le Jurassique du Portugal Esquisse stratigraphique et zonale. Boletim Sociedade Geológica de Portugal 18, 73-104.

Mouterde, R., Rocha, R.B., Ruget, C., Tintant, H., 1979. Faciès, biostratigraphie et paléogéographie du Jurassic portugais. Ciências da Terra (U.N.L.) 5, 29-52.

Nederbragt, A.J., Fiorentino, A. 1999. Stratigraphy and palaeoceanography of the Cenomanian-Turonian Boundary Event in Oued Mellegue, north-western Tunisia. Cretaceous Research 20, 47-62.

Noël, D., 1965. Sur les coccolithes du Jurassique européen et d'Afrique du Nord. Essai de classification des coccolithes fossiles. Edition du Centre National de la Recherche Scientifique, Paris, 1-209.

O'Dogherty, L., Sandoval, J., Bartolini, A., Bruchez, S., Bill, M., Guex, J., 2006. Carbon-isotope stratigraphy and ammonite faunal turnover for the Middle Jurassic in the Southern Iberian palaeomargin. Palaeogeography, Palaeoclimatology, Palaeoecology 239, 311-333.

Pavia, G., Enay, R., 1997. Definition of the Aalenian-Bajocian Stage boundary. Episodes 20, 16-22.

Perch-Nielsen, 1968. Der Feinbau und die Klassifikation der Coccolithen aus dem Maastrichtien von Dänemark. Det kongelige Danske Videnskabernes Selskab Biologiske Skrifter 16, 1-96.

Perch-Nielsen, K., 1985. Mesozoic calcareous nannofossils. In: Bolli, H.M., Saunder, J.B., Perch-Nielsen, K. (Eds.). Plankton Stratigraphy, Cambridge, 329-426.

Premoli Silva, I., Erba, E., Tornaghi, M.E., 1989. Paleoenvironmental signals and changes in surface fertility in Mid Cretaceous C_{org}-Rich pelagic fcies of the Fucoid Marls (Central Italy). Geobios 11, 225-236.

Price, G.D., 2010. Carbon-isotope stratigraphy and temperature change during the Early-Middle Jurassic (Toarcian-Aalenian), Raasay, Scotland, UK. Palaeogeography, Palaeoclimatology, Palaeoecology 285, 255-263.

Reale, V., Baldanza, A., Monechi, S., Mattioli, E., 1992. Calcareous nannofossil biostratigraphic events from the Early-Middle Jurassic of the Umbria-Marche area (Central Italy). Memoire della Società Geologica di Padova 42, 41-75.

Redner, R.A., Walker, H.F., 1984. Mixture densities, maximum likehood and the EM algorithm. SIAM Review 26, 195-239.

Ribeiro, A., Antunes, M.T., Ferreira, M.P., Rocho, R.B., Soares, A.F., Zbyszewski, G., de Almeida, F.M., de Carvalho, D., Monteiro, J.H., 1979. Introduction à la géologie générale du Portugal, Serviço Geológico de Portugal. Lisboa, 114 p.

Rocha, R.B., Manupella, G., Mouterde, R., Ruget, C., Zbyszewski, G., 1981. Carta Geológica de Portugal na escala de 1/50000. Notícia explicativa da folha 19-C, Figueira da Foz. Serviço Geológico de Portugal. Lisboa, 1-126.

Rocha, R.B., Henriques, M.H., Soares, A.F., Mouterde, R., Caloo, B., Ruget, C., Fernández-López, S., 1990. The Cabo Mondego section as a possible Bajocian boundary stratotype. Memoria per servire alla Descrizione della Carta Geologica d'Italia, Roma, XL; 49-60.

Ruget-Perrot, C., 1961. Études stratigraphiques sur le Dogger et le Malm inférieur du Portugal au Nord du Tage, Bajocien, Bathonien, Callovien, Lusitanien. Memórias dos Serviços Geológicos de Portugal 17, 1-197.

Roth, P.H., 1973. Calcareous Nannofossils, Leg 17 – Deep Sea Drilling Project. In: Winterer, E.L., Ewing, J.I., et al., (Eds.). Initial Reports of the Deep Sea Drilling Project, Washington, 17, 695-795.

Roth, P.H., 1978. Cretaceous Nannoplankton biostratigraphy and oceanography of the northwestern Atlantic Ocean. In Benson, W.E., Sheridan, R.E., et al., (Eds.). Initial Reports of the Deep Sea Drilling Project, Washington, 44, 731-759.

Roth, P.H., Thierstein, H.R., 1972. Calcareous nannoplankton: Leg 14 of the Deep Sea Drilling Project. In Hayes, D.E., Pimm, A.C., et al., (Eds.). Initial Reports of the Deep Sea Drilling Project, Washington, 14, 421-486.

Sandoval, J., O'Dogherty, L., Guex, J., 2001. Evolutionary rates of Jurassic ammonites in relation to sea-level fluctuations. Palaios 16, 330-363.

Sandoval, J., O'Dogherty, L., Vera, J.A., Guex, J., 2002. Sea level changes and ammonite faunal turnover during the Lias/Dogger transition in the western Tethys. Bulletin de la Société Géologique de France 173, 57-66.

Sandoval, J., O'Dogherty, L., Aguado, R., Bartolini, A., Bruchez, S., Bill, M., 2008. Aalenian carbon-isotope stratigraphy: Calibration with ammonite, radiolarian and nannofossil events in the Western Tethys. Palaeogeography, Palaeoclimatology, Palaeoecology 267, 115-137.

Suan, G., Mattioli, E., Pittet, B., Mailliot, S., 2008. Evidence for major environmental perturbation prior to and during the Toarcian (Early Jurassic) oceanic anoxic event from the Lusitanian Basin, Portugal. Paleoceanography 23. doi:10.1029/2007PA001459.

Suan, G., Mattioli, E., Pittet, B., Lécuyer, C., Suchéras-Marx, B., Duarte, L.V., Philippe, M., Reggiani, L., Martineau, F., 2010. Secular environmental precursors to Early Toarcian (Jurassic) extreme climate changes. Earth and Planetary Science Letters 290, 448-458.

Suchéras-Marx, B., Mattioli, E., Pittet, B., Escarguel, G., Suan, G., 2010. Astronomically-paced coccolith size variations during the early Pliensbachian (Early Jurassic). Palaeogeography, Palaeoclimatology, Palaeoecology 295, 281-292.

Suchéras-Marx, B., Guihou, A., Giraud, F., Mattioli, E., Lécuyer, C., Pittet, B., 2011. The Middle Jurassic Watznaueria (coccolith-type algae), diversification impact on carbon cycle

and bulk carbonate composition. EGU General Assembly. Vienna. Geophysical Research Abstracts 13, EGU2011-454.

Tiraboschi, D., Erba, E., 2010. Calcareous nannofossil biostratigraphy (upper Bajocian-lower Bathonian) of the Ravin du Bes section (Bas Auran, Subalpine Basin, SE France); evolutionary trends of *Watznaueria barnesiae* and new findings of *Rucinolithus* morphotypes. Geobios 43, 59-76.

Titterington, D., Smith, A., Makov, U., 1985. Statistical analysis of finite mixture distributions. John Wiley & Sons. Chichester, UK. 243 p.

Trammer, J., 2002. Power formula for Cope's rule. Evolutionary Ecology Research 4, 147-153.

Trammer, J., 2005. Maximum body size in a radiating clade as a function of time. Evolution 59, 941-947.

Tremolada, F., Van de Schootbrugge, B., Erba, E., 2005. The Early Jurassic Schizosphaerellid crisis: implications for calcification rates and phytoplankton evolution across the Toarcian OAE in Cantabria, Spain. Paleoceanography 20. doi:10.1029/2004PA001120.

Tremolada, F., Erba, E., 2002. Morphometric analyses of Aptian *Assipetra infracretacea* and *Rucinolithus terebrodentarius* nannoliths: implications for taxonomy, biostratigraphy and paleoceanography. Marine Micropaleontology 44, 77-92.

Watkins, D.K., 1989. Nannoplankton productivity fluctuations and rhythmically-bedded pelagic carbonates of the Greenhorn Limestone (Upper Cretaceous). Palaeogeography, Palaeoclimatology, Palaeoecology 74, 75–86

Watkinson, M.P., 1989. Triassic to Middle Jurassic sequences from the Lusitanian Basin, Portugal, and their equivalents in other North Atlantic margin basins. Unpubl. PhD Thesis, The Open University, Milton Keynes, 390 p.

Wilson, R.C.L., 1988. Mesozoic development of the Lusitanian Basin, Portugal. Revista de la Sociedad Geológica de España 1, 393-407.

Wilson, R.C.L., Hiscott, R.N., Willis, M.G., Gradstein, F.M., 1989. The Lusitanian Basin of West-Central Portugal: Mesozoic and Tertiary tectonic, stratigraphic and subsidence history. AAPG Memories 46, 341-361.

Table captions

Table 1. Statistics of measured parameters of *Discorhabdus* in the Cabo Mondego section.

Table 2. Correlation between the different biometric parameters measured in natural light for the *Discorhabdus* pool.

Table 3. Size ranges of different *Discorhabdus* morpho-species as reported in the literature and in this study.

Figure captions

Figure 1. Location of the Cabo Mondego section. a) Present-day location. b) Paleogeography of western Tethys during the Bajocian-Bathonian interval re-drawn after Ziegler (1988).

Figure 2. a) Polarized (i) and natural (ii) light images of the three morpho-species of *Discorhabdus* recognized in this work. Photograps are taken under light microscope. b) The biometric parameters measured: L and l axis of distal/proximal shields and of central area. Radial elements are also shown. Scale bar = 2 μm.

Figure 3. The nannofossil and *Discorhabdus* accumulation rates, and *Discorhabdus* percentages are compared to the biometric results and to the $\delta^{13}C$ profil of Cabo Modego section. The codes of the samples analyzed for biometry are in black, while the codes of the samples in grey correspond to supplementary samples studied for abundances, accumulation rates and $\delta^{13}C$.

Figure 4. Results of mixture analysis applied to distal and proximal shields, and of central area of the *Discorhabdus* pool after measurements in natural ligth. Scale bar = 2 μm.

Figure 5. Compilation of $\delta^{18}O$ and $\delta^{13}C$ values from some Mediterranean Tethys settings plotted against biometric results from Cabo Mondego section. The decrease in $\delta^{18}O$ values attests a temperature increase from Concavum to Sauzei Zones. $\delta^{13}C$ values increase passing from Concavum to Sauzei Zones, probably indicating an increase in productivity.

Figure 1

Click here to download Figure(s): LOPEZ-OTALVARO_ETAL_Fig1.eps

a)

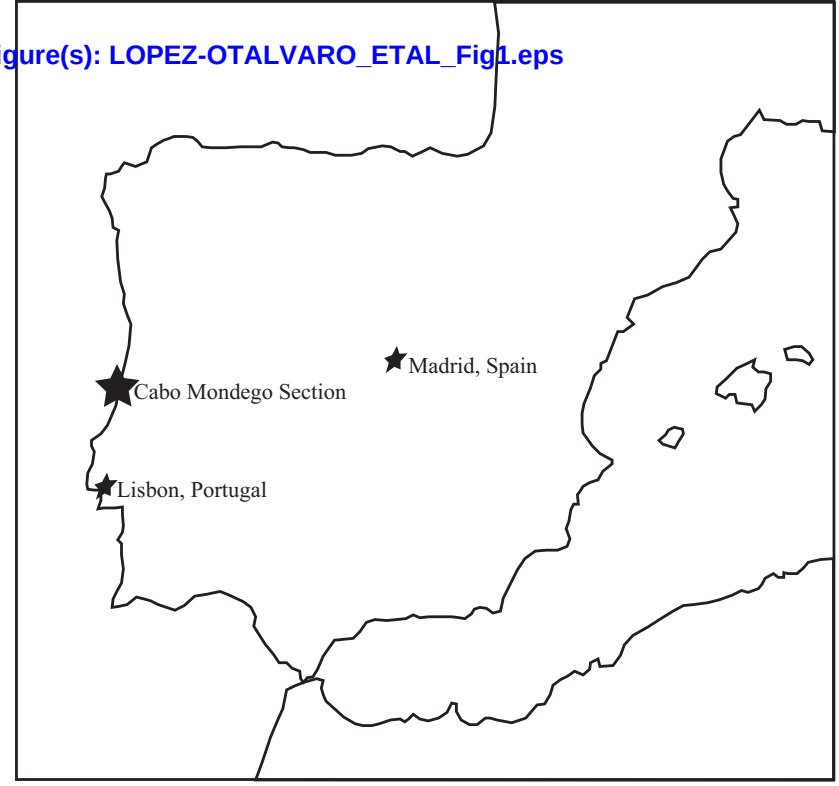

b)

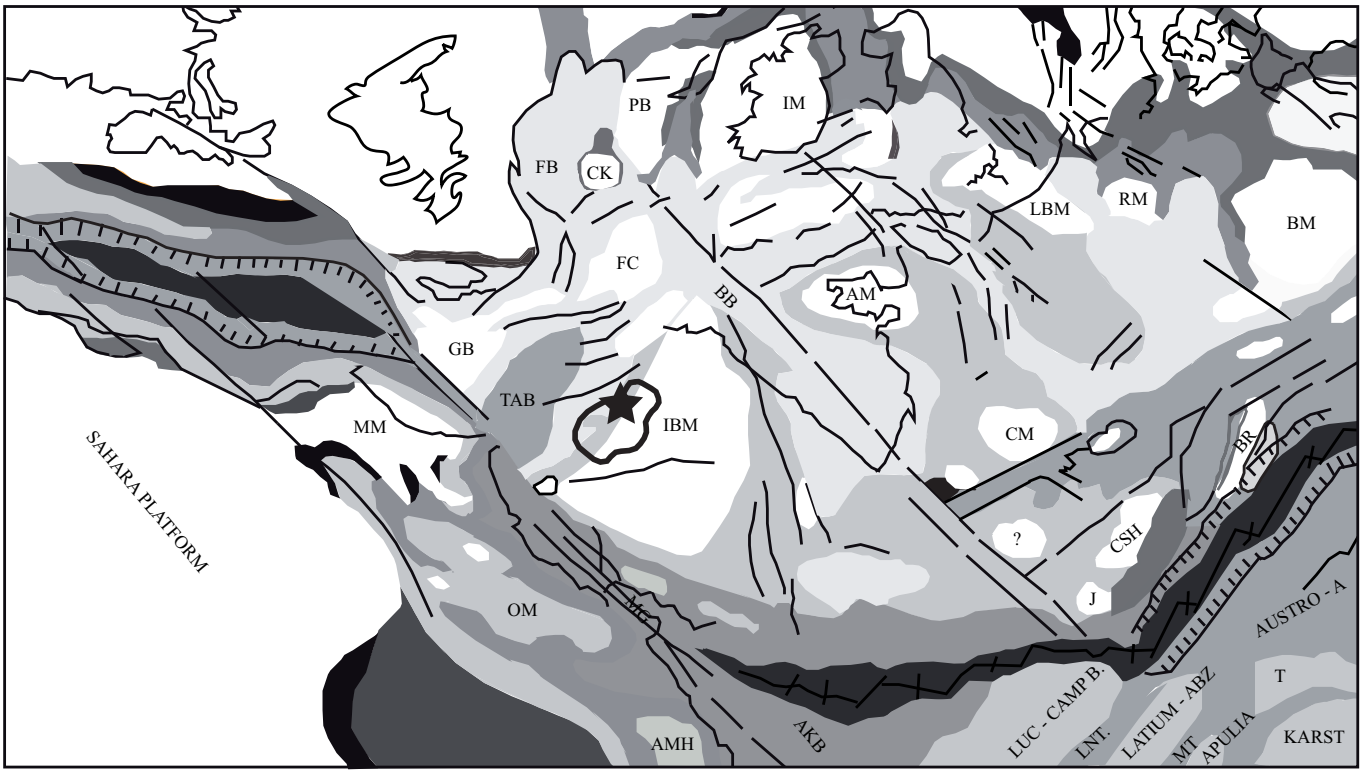

- mainly continental clastics
- deltaic-shallow marine, mainly sands
- shallow marine, mainly shales
- shallow marine, carbonates and clastics
- shallow marine, mainly carbonates
- Evaporites, clastics and carbonates
- Evaporites and carbonates
- Deeper marine clastics and/or carbonates
- Deeper marine, mainly sands (flysch)
- Basins floored by oceanic crust

- Anorogenic, cratonic
- Active sea-floor spreading axis
- Faults, wrench, normal
- Continental slope

AKB ALBORAN-KABYLIAN BLOCK
AM ARMORICAN MASSIF
AMH AIN M`LILA HIGH
AUSTRO ALP AUSTRO ALPINE BLOCK
BB BAY OF BISCAY RIFT
BM BOHEMIA MASSIF
BR BRIANCONNAIS
CSH CORSICA-SARDINA HIGH
FB FUNDY BASIN
FC FLEMISH CAP
GB GRAND BANKS
IBM IBERIA MESETA
IM IRISH MASSIF LBM LONDON-BRABANT MASSIF
J JULIAN PLATFORM
LNT LAGONEGRO TROUGH
LUC. CAMP. B. LUCANIA-CAMPANIA BLOCK
MC MASSIVE CENTRAL
MG MAGHREBIAN-GIBRALTAR RIFT
MT MOLISE TROUGH
MM MAROCCO-MESETA
OM ORAN MESETA
RM RHENISH MASSIF
T TRENTO PLATFORM
TAB TAGUS ABYSSAL PLAIN

Cabo Mondego Section

Lusitanian Basin

Figure 2

Click here to download Figure(s): LOPEZ-OTALVARO_ETAL_Fig2.eps

a)

i

ii

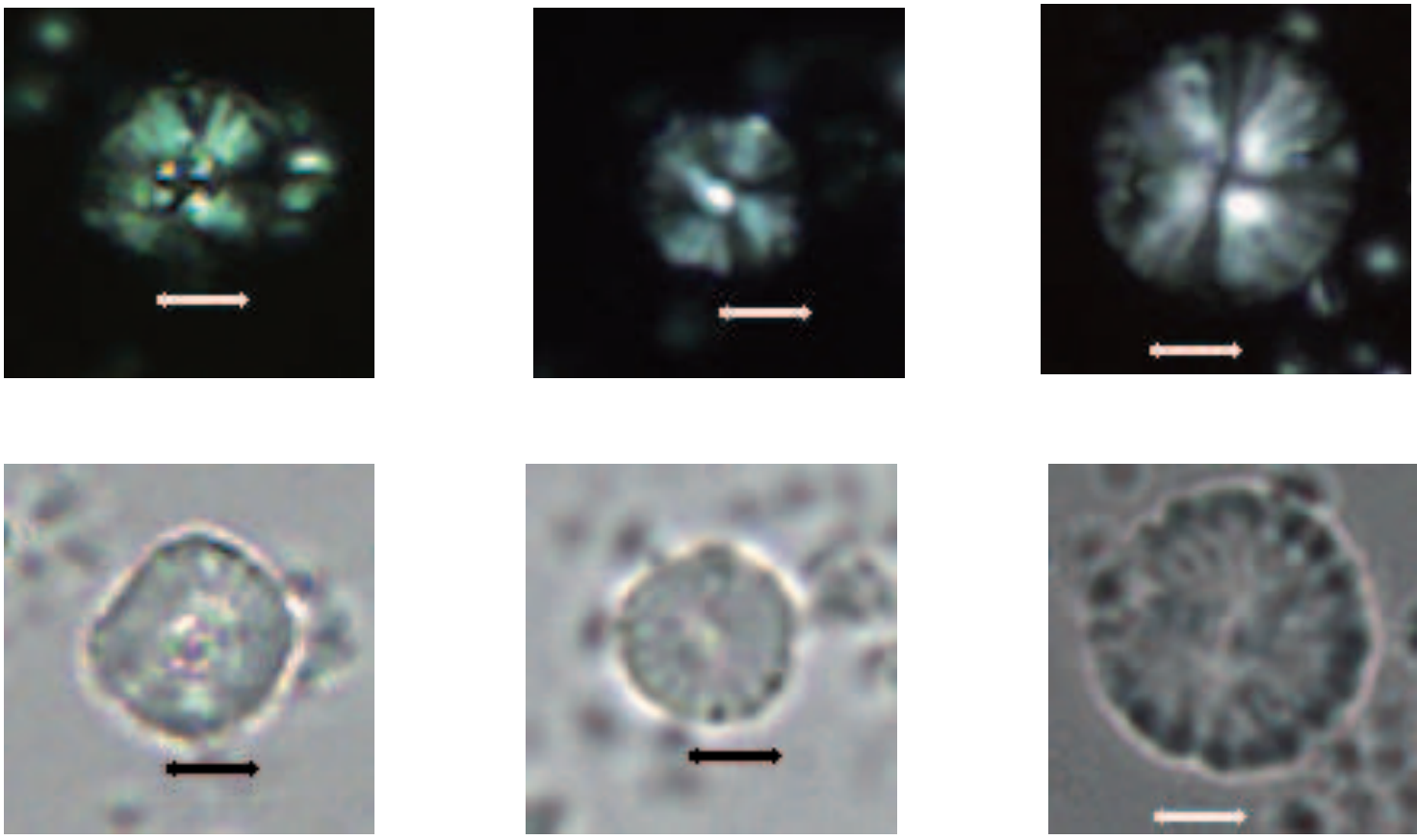

D. criotus
sample CM15

D. ignotus
sample CM29

D. striatus
sample CM10

b)

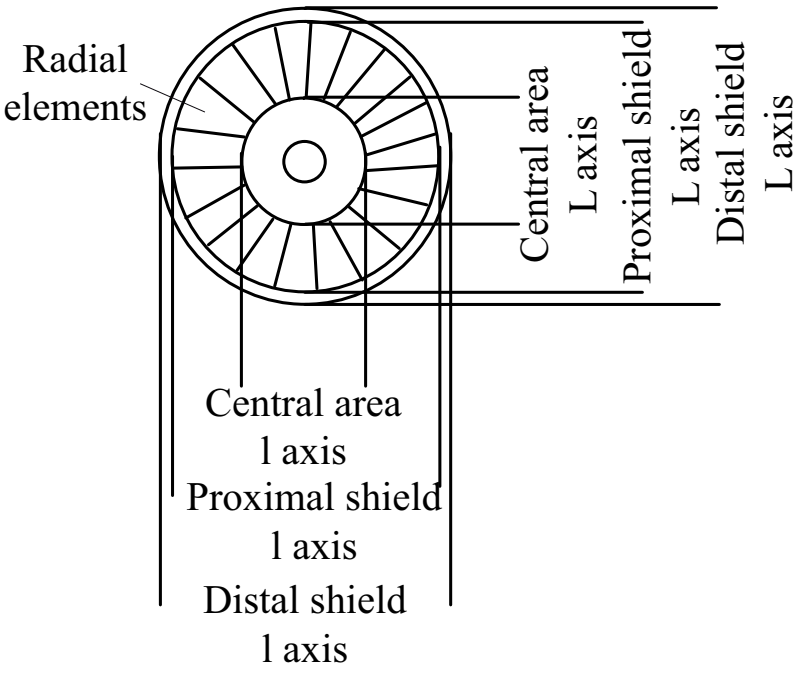

Figure 3

Click here to download Figure(s): LOPEZ-OTALVARO_ETAL_Fig3.eps

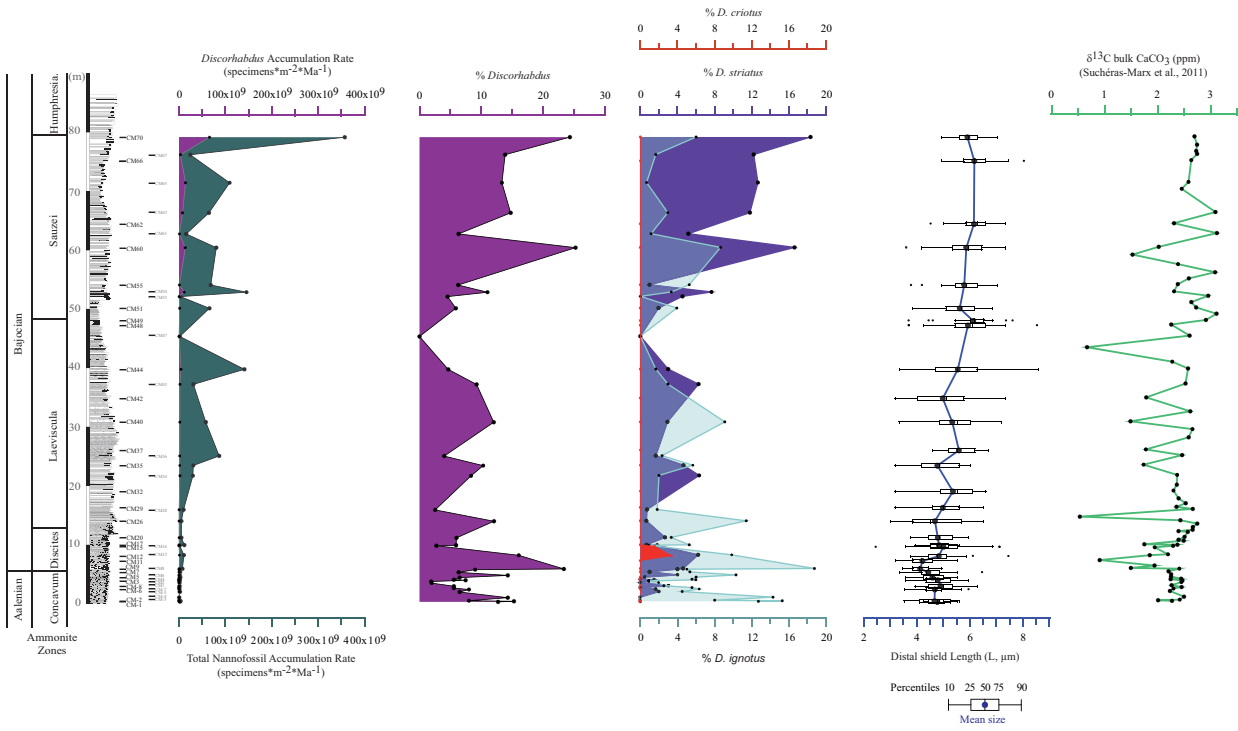

Figure 4

Click here to download Figure(s): LOPEZ-OTALVARO_ETAL_Fig4.eps

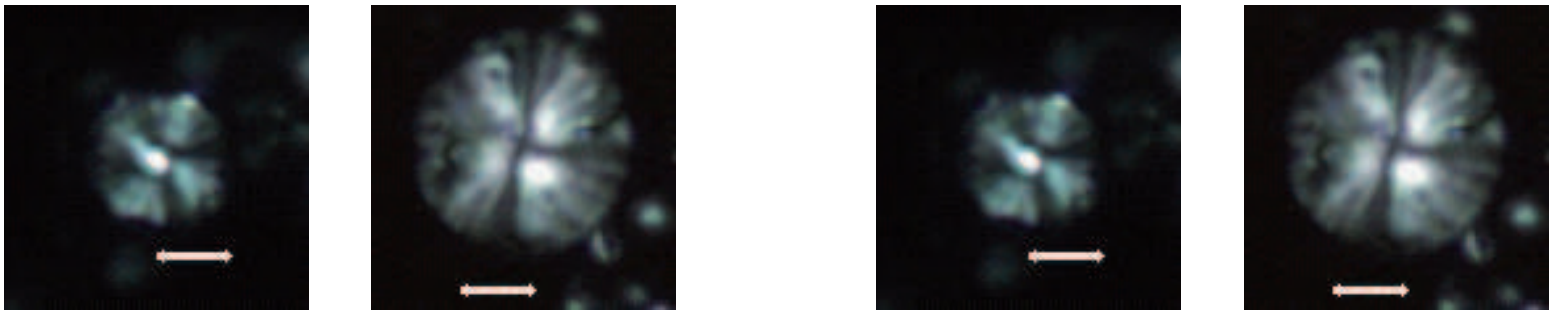

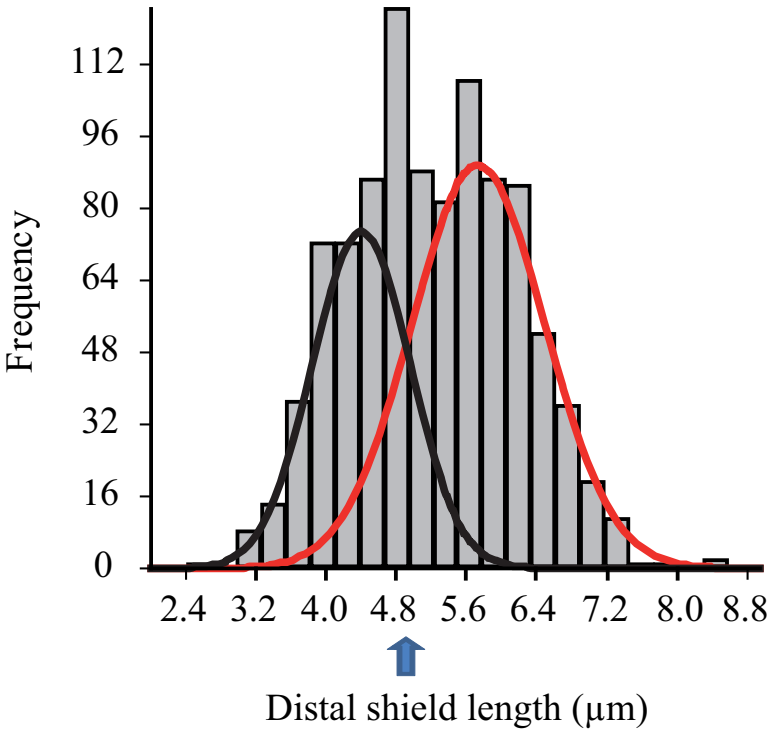

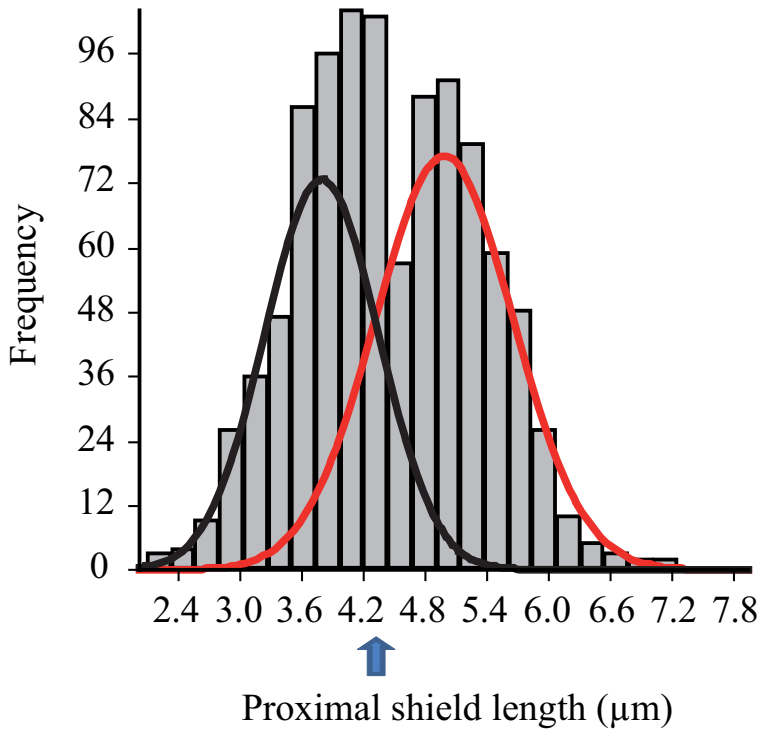

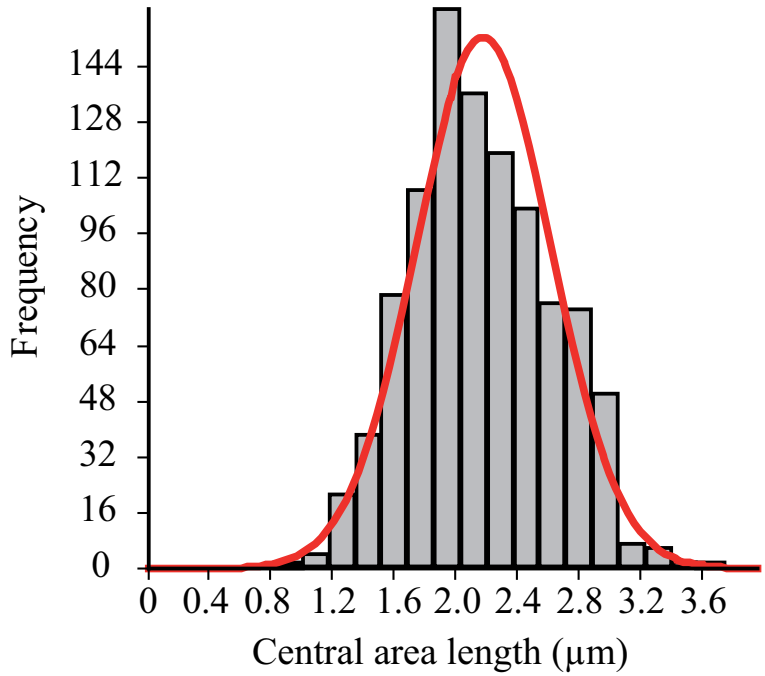

Figure 5

Click here to download Figure(s): LOPEZ-OTALVARO_ETAL_Fig5.eps

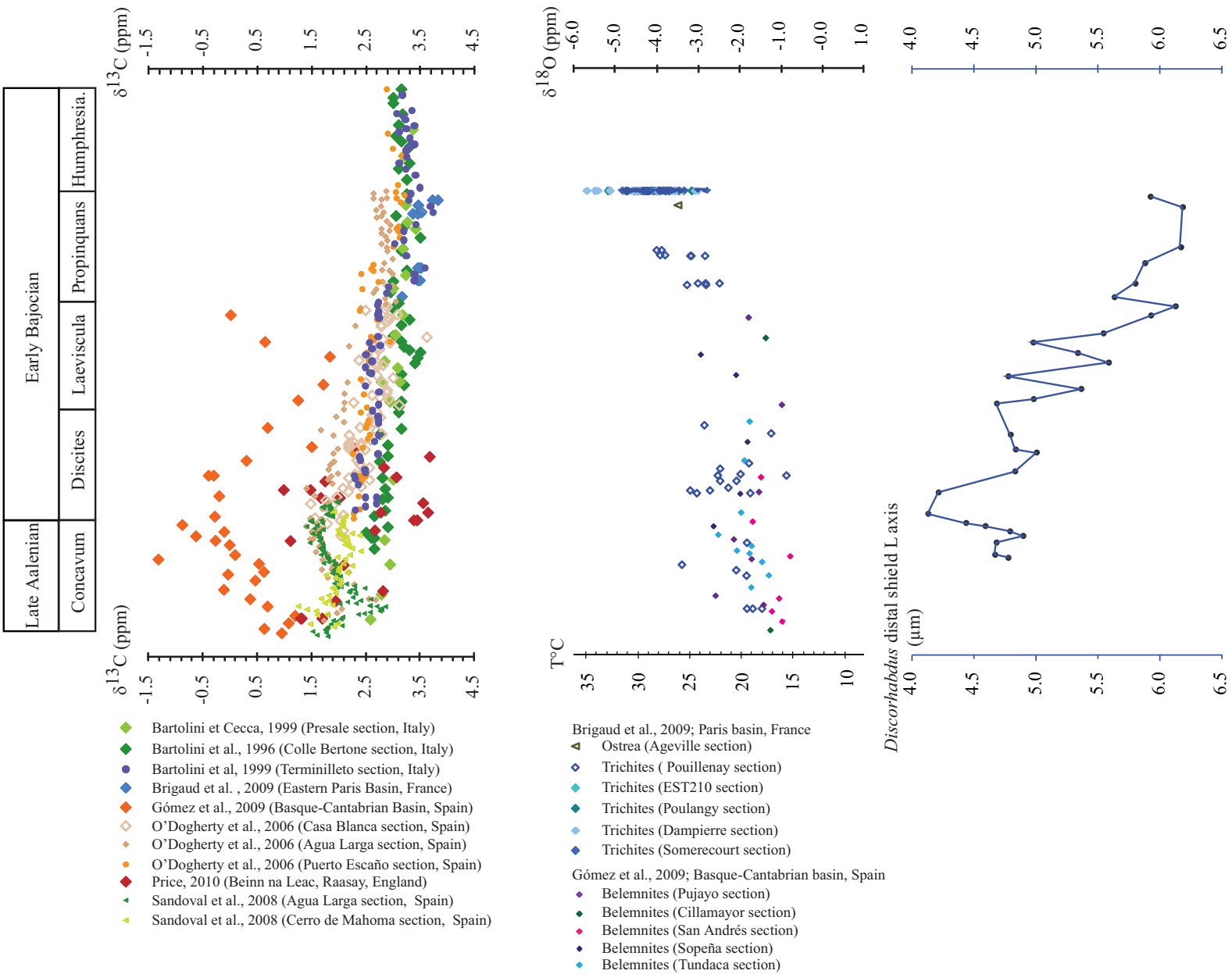

Table 1

		Distal shield L axis (µm)	Distal shield l axis (µm)	Distal shield ellipticity (coccolith ellipticity)	Proximal shield L axis (µm)	Proximal shield l axis (µm)	Central area L axis (µm)	Central area l axis (µm)	central area proportion / distal shield
Discorhabdus ignotus	Mean	4.31	4.13	0.96	3.65	3.48	1.82	1.74	42.18
	Median	4.42	4.17	0.97	3.67	3.50	1.83	1.75	41.92
	Minimum	2.42	2.33	0.79	2.08	2.00	0.83	0.83	25.55
	Maximum	4.92	4.92	1.00	4.50	4.42	2.58	2.42	59.31
	Standar deviation	0.45	0.46	0.04	0.44	0.44	0.27	0.26	4.57
	Number of measurements	412	412	412	412	412	412	412	412
Discorhabdus striatus	Mean	5.88	5.66	0.96	5.04	4.84	2.44	2.34	41.52
	Median	5.83	5.63	0.97	5.00	4.83	2.42	2.33	41.59
	Minimum	5.00	4.17	0.83	3.83	3.50	1.50	1.42	25.29
	Maximum	8.58	8.08	1.00	7.25	6.92	3.75	3.58	57.12
	Standar deviation	0.62	0.64	0.03	0.58	0.58	0.35	0.34	4.77
	Number of measurements	570	570	570	570	570	570	570	570
Discorhabdus criotus	Mean	4.84	4.84	1.00	4.13	4.13	2.46	2.42	50.88
	Median	4.84	4.84	1.00	4.13	4.13	2.46	2.42	50.88
	Minimum	4.75	4.75	1.00	3.92	3.92	2.42	2.42	50.81
	Maximum	4.92	4.92	1.00	4.33	4.33	2.50	2.42	50.95
	Standar deviation	0.12	0.12	0.00	0.29	0.29	0.06	0.00	0.10
	Number of measurements	2	2	2	2	2	2	2	2

Table 2

	Distal shield "L"	Proximal shield (L)	
Number of elements	0.534 <0.0001	0.524 <0.0001	N=881
Distal shield "L"	0.981 <0.0001		N=984
Central area "L"	0.825 <0.0001		N=984
Central area "l"	0.825 <0.0001		N=984
Proximal shield "l"		0.979 <0.0001	N=984
Central area "L"		0.828 <0.0001	N=984
Central area "l"		0.828 <0.0001	N=984

Table 3

Species	Size range	Interval	Original diagnosis/description	Reference
D. striatus	5.00-8.58	Late Aalenian to Early Bajocian	This study	This study
D. striatus	5.50-7.00	Lias	Moshkovitz and Ehrlich, 1976	Moshkovitz and Ehrlich, 1976
D. striatus	5.00-7.00	Aalenian	Moshkovitz and Ehrlich, 1976	Reale et al., 1992
D. aff. *striatus*	6.00-8.00	Toarcian-Early Bajocian	Moshkovitz and Ehrlich, 1976	Cobianchi, 1992
Tremalithus ignotus	5.00	Upper Maastrichtian	Gorka, 1957	Gorka, 1957
D. ignotus	2.42-5.00	Late Aalenian to Early Bajocian	This study	This study
D. ignotus	4.00-5.00	Lower Maastrichtian	Perch-Nielsen, 1968	Perch-Nielsen, 1968
D. ignotus	3.50-6.40		Perch-Nielsen, 1968	Bown, 1987a
D. ignotus	3.50-5.50	Early-Middle Jurassic	Perch-Nielsen, 1968	Reale et al., 1992
Bidiscus ignotus	2.50-5.50	Berriasian, Hauterivian	Gorka, 1957	Grün and Allemann, 1975
Bidiscus ignotus	2.50-5.00	Tithonian	Gorka, 1957 (Haumman, 1970)	Keupp, 1976
Bidiscus ignotus	2.30-5.00 (7.00)	Tithonian	Gorka, 1957 (Haumman, 1970)	Keupp, 1977
D. criotus	3.60-5.60		Bown, 1987a	Bown, 1987a